FORSCHUNGSZENTRUM
ROSSENDORF e.V.

FZR

FZR 93 - 15
May 1993

INSTITUTE OF RADIOCHEMISTRY

Annual Report 1992

Editor: Dr. Gert Bernhard

Annual Report 1992

Institute of Radiochemistry

Editor: Dr. G. Bernhard

Redaction: Dr. H.-J. Engelmann
Dr. G. Geipel

CONTENTS

I. INTRODUCTION 1

II. SCIENTIFIC CONTRIBUTIONS 5

1. COMMON RESEARCH 7

PROBLEMS OF PENETRATING IODINE SPECIES IN A NUCLEAR-CHEMICAL PLANT 9
G. Bernhard

A KINETIC STUDY ON THE ROLE OF COMPLEX FORMATION IN THE ION EXCHANGE SEPARATION OF RARE EARTHS BY MEANS OF DTPA 12
L. Baraniak

A KINETIC ANALYSIS OF THE ION EXCHANGE PROCESSES OF TERVALENT RARE-EARTHS-DTPA COMPLEXES 14
L. Baraniak, H.-J. Engelmann

ION EXCHANGE SEPARATION OF TRACE AMOUNTS ADJACENT RARE EARTHS FROM GADOLINIUM BY MEANS OF NITRILOTRI-ACETIC ACID 17
L. Baraniak, H.-J. Engelmann

STEADY STATE OXYGEN ACTIVITIES AT SILVER SURFACES IN REACTING OXYGEN-HYDROGEN MIXTURES 19
D. Rettig

IN-LINE OXIDATION STUDIES OF METALS 24
C. Nebelung, D. Rettig

SPAREX - A NEW EXPERIMENTAL LOOP FOR INVESTIGATING THE TRANSPORT BEHAVIOUR OF RADIOTOXIC AND TOXIC GASBORNE CHEMICAL SPECIES 29
P. Griepentrog, P. Merker, D. Rettig, H. Stöbel,
W. Witge, H. Zänker

THE SCIENTIFIC STRATEGY OF THE SPAREX EXPERIMENTS FOR THE NEXT TWO YEARS 32
H. Funke, P. Griepentrog, G. Hüttig, P. Merker, D. Rettig, H. Stöbel, W. Witge, H. Zänker

2. CHEMISTRY OF HEAVY ELEMENTS 39

GAS CHROMATOGRAPHIC STUDIES OF MOLYBDENUM OXIDES AND HYDROXIDES 41
S. Hübener, A. Roß, B. Eichler, H. W. Gäggeler, J. Kovacs, S. N. Timokhin, A. B. Yakushev

SEPARATION OF CARRIER-"FREE" MOLYBDENUM FROM ZIRCONIUM 43
A. Roß, S. Hübener

VOLATILIZATION AND GAS PHASE TRANSPORT OF ELEMENT 106 IN HUMID OXYGEN 46
B. Eichler, H. W. Gäggeler, S. Hübener

THERMOCHROMATOGRAPHY OF CALIFORNIUM, EINSTEINIUM, AND FERMIUM IN METALLIC COLUMNS 49
S. Hübener, B. Eichler, H. W. Gäggeler, M. Schädel

3. ECOLOGICAL RESEARCH 53

MINING RELICS AS SOURCES OF NATURAL RADIOACTIVITY II. RELEASE OF RADON FROM URANIUM MILL TAILINGS 55
L. Baraniak, A. Mende

ACID FORMATION BY AUTOXIDATION OF SULPHIDE ORES AND THE INFLUENCE ON THE SOLUBILITY OF ORE COMPONENTS 57
H.-J. Engelmann

A SIMPLE BALANCE FOR WEATHERING OF ROCKS IN A ROCKPILE 59
G. Geipel

INVESTIGATIONS OF THE SOLUBILITY OF HEAVY METALS CONTAINED IN ROCKPILE MINERALS 61
G. Geipel

DISTRIBUTION OF SOME RADIONUCLIDES IN THE ROCKPILE 250 IN SCHLEMA 63
G. Geipel

BATCH TESTING WITH INTEGRATED ANALYSIS - INTERACTION BETWEEN LEAD IONS AND GRANODIORITE 65
M. Thieme

CHEMOMETRIC ANALYSIS OF THE SPECTROPHOTOMETRIC DETERMINATION OF LEAD IN THE PRESENCE OF IRON(II) 67
M. Thieme

A MODERNIZATION OF THE ZEISS M80 INFRA-RED SPECTROMETER 69
R. Nicolai, K.-H. Heise

SINGLE-STEP-SYNTHESIS OF [1,2-^{14}C]TRICHLORO-ACETIC ACID STARTING FROM [1,2-^{14}C]POTASSIUM ACETATE 71
M. Bubner, K.-H. Heise, V. Vlasakova, K. Fuksova

CHARACTERIZATION AND INVESTIGATION OF REACTIVITY OF HUMIC SUBSTANCES WITH RADIOTRACERTECHNIQUE - SUMMARY OF A STUDY 76
M. Bubner, K.-H. Heise

III. PUBLICATIONS, LECTURES AND POSTERS 83

IV. TALKS OF VISITORS 89

V. PERSONNEL 95

VI. ACKNOWLEDGEMENTS 99

I. INTRODUCTION

Introduction

The Institute for Radiochemistry of the Research Center Rossendorf Inc. (FZR) started its work on 1 January 1992.
As part of the FZR the Institute of Radiochemistry (IRC) is supported by the Free State of Saxony and the Federal Republic of Germany on the basis of equal shares. Futhermore the IRC has experienced helpful support in form of additional grants.

This Annual Report summerizes the research activities achieved in the first year. But it must be remarked that some papers result from research activities are done in the different divisions of radiochemisty of the former Nuclear Research Centre Rossendorf.

Problems of radioecology influence the present research programm and profile of this institute.
The major goal of the IRC is fundamental and applied research on the field of the transport behaviour of radiochemical pollutants in the biosphere.
Owing to the fact that Saxony and Thuringia are partly contaminated from previous uranium mining activities these investigations are of actual importance.

In future the research work will be focussed on the following topics:
- transport of radionuclides
  * solubility and speciation of radionuclides
  * model of solubility
  * formation and distribution of colloids and aerosols
  * sorption of radionuclides
  * transport model of the pollutants
- experiments with synchrotron radiation
- bioremediation
- analysis of traces

An essential prerequisite for a further successful scientific research work and a helpful cooperation with the university was fulfilled by the vocation of Dr. H. Nitsche (presently at Lawrence Berkeley Lab., Berkeley, U.S.) as director of IRC and professor at the Department of Chemistry of the Technical University Dresden.

G. Bernhard
Acting Director of the
Institute of Radiochemistry

II. SCIENTIFIC CONTRIBUTIONS

1. COMMON RESEARCH

PROBLEMS OF PENETRATING IODINE SPECIES IN A NUCLEAR-CHEMICAL PLANT

G. Bernhard
Research Center Rossendorf Inc., Institute of Radiochemistry

Because of their smallest amounts, it is very difficult to identify the so-called penetrating iodine species orginating in nuclear plants.
It is assumed that these compounds are formed by the reaction of radioactive iodine with different organic materials of the plant (cables, lubricants, plastics). There are discussed aromatic iodine compounds but as a further inorganic species the free hypoiodic acid is postulated.
The presence of such penetrating substances can be seen by a lower efficiency of the used filter materials.
The efficiency can be characterized by the decontamination factor (DF):

$$DF = \frac{\textit{iodine activity before filter unit}}{\textit{iodine activity after filter unit}} \qquad (1)$$

Normally, $CH_3{}^{131}I$ and $^{131}I_2$ are used for deciding the DF-value of a filter unit.
In nuclear-chemical plants silicagel impregnated with silver nitrate is utilized as an iodine sorption material /1/.
In dependence on the parameters of the gas flow and filter design the DF-value of CH_3I is in the range of $5*10^3$ - 10^5.
In dissolution process of irradiated fuel with nitric acid iodine is distributed between the aqueous (I^-, IO_3^-, IO_4^-) and the gas phase (HI, I_2).
The ratio of the distribution depends on the oxidising or reducing conditions, the concentration of iodine, and the efficiency of the reflux of iodine with the condensate /2/.
During this dissolving process more than 90% of iodine can be released to the off-gas and then separated by washing out or chemisorption.

In the AMOR-I plant /3/ ordinary fuel elements of a research reactor were reprocessed for fission molybdenum production.

After using this fuel element for 200 h it was unloaded and stored for cooling over about 48 h. At the time of dissolution the activity of iodine is $1.01*10^{14}$ Bq ($2.4*10^{13}$ Bq ^{131}I, $4.6*10^{13}$ Bq ^{132}I and $3.1*10^{13}$ Bq ^{133}I). The produced amount of fission iodine is 9.3 mg and the resulting concentration in the fuel element solution is $3.6*10^{-6}$ mol I/L.

The removal of iodine is based of a two-barrier system (Fig. 1). After passing through an iodine filter (1) the off-gas of all apparatuses (2,3,4,5) streams into the atmosphere of the hot cell. The air of the cell was completely purified from the iodine contamination by a safety iodine filter unit (6) and an aerosol filter unit (7). Both iodine filter units are filled with silicagel impregnated with silver nitrate. The temperature of the filter material is about 130°C. The iodine activities in the off-gas

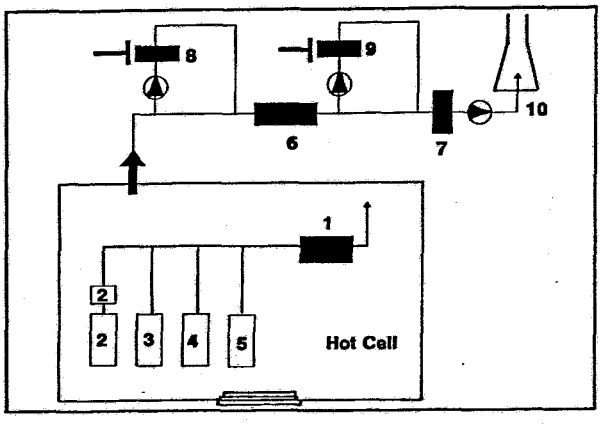

Fig. 1:
Scheme of iodine removal

1 iodine filter,
2 dissolver with additional filter unit,
3 air-lift mixer,
4 centrifuge,
5 vessels,
6 safety iodine filter unit,
7 aerosol filter unit,

before and after the safety filter unit can be measured by a bypass filter system (8/9). The preparation and the properties of the used control filter "RICO" have been described in detail elsewhere /4/. So the decontamination factor of the safety iodine filter unit can be determined under original processing conditions.
The DF of $CH_3{}^{131}I$ released in the hot cell was in the range of $5*10^3$ - $2*10^4$ depending on the accumulated working time of the safety filter unit. During the operation of the plant (dissolution, fission molybdenum separation by ion exchange in an air lift mixer/centrifuge-system) the DF of iodine contaminants in the cell atmosphere was decided to $3.0*10^2$.
That means the DF of iodine contaminants orginated from the process is lower than that of $CH_3{}^{131}I$.
Following to this fact it can be assumed that penetrating iodine forms orginate in this plant.

To dissolve aluminium cladded fuel elements with nitric acid it is necessary to add mercury as a catalyst /5/.
The HNO_3 contains $1*10^{-3}$ mol Hg/L. According to the solubility product of HgI_2 ($3.2*10^{-29}$) /6/ the formation of mercury iodide is possible.
The experiments have shown that mercury iodide is formed under original conditions /7/. The formation of mercury iodide is the reason that about 90% of iodine activity is in the fuel element solution after dissolution and fission molybdenum separation process.
So it had to be investigate in a laboratory scale the decontamination factor of HgI_2 on the silver nitrate impregnated silicagel.
The release of HgI_2 into the cell air is given by leaks of the process containment or by passing the iodine process filter units (low decontamination factor) in form of aerosols or gaseous.
To simulate the original mixing process for molybdenum separation (see Fig.2) air streams through a simulated fuel element solution (1) (1.6 mol/L $Al(NO_3)_3$, $2.2*10^{-2}$ mol/L $UO_2(NO_3)_2$) containing $^{203}HgI_2$ or $Hg^{131}I_2$ (concentration $1*10^{-3}$ mol/L). In further experiments $K^{131}I$ activity is added to this solution. The test tube (2) is filled with silicagel impregnated with silver nitrate.
The decontamination factor of the used control filters (3,4) tested with HgI_2 was $1.0*10^4$ and tested with CH_3I it was $5*10^4$.
So it was sure that all HgI_2 is deposited at the control filter system (3).

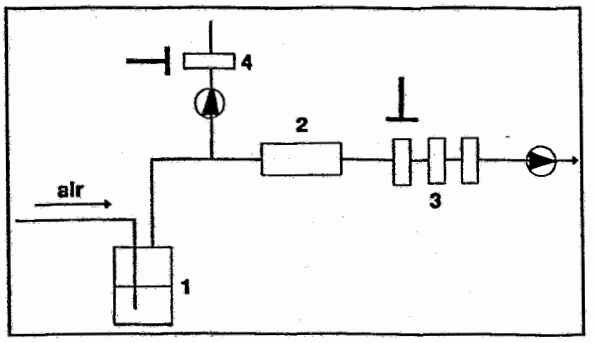

Fig.2:
Determination of DF factor

1 vessel with fuel element solution,
2 test tube with silver nitrate impregnated silicagel,

Under experimental conditions the DF of HgI_2 aerosol/gaseous on the Ag-silicagel-filter material was in average $1.3*10^2$ but that of KI $3.3*10^4$.
According to these experiments it can be concluded that in the AMOR-I plant HgI_2 is one penetrating iodine species.

References

/1/ R. Schwarzbach, G. Bernhard, W. Boeßert, O. Hladik
Kernenergie 28, 92 (1985)
/2/ G. Koch, W. Ochsenfeld, H. Schmieder, W. Weinländer
Kerntechnik 18, 253 (1976)
/3/ R. Münze, O. Hladik, G. Bernhard, W. Boeßert, R. Schwarzbach
Int.J. Appl. Radiat. Isot. 35, 749 (1984)
/4/ R. Schwarzbach, O. Hladik
Kernenergie 27, 25 (1984)
/5/ G. Bernhard, W. Boeßert, O. Hladik, R. Schwarzbach
Kernenergie 27, 27 (1984)
/6/ M.S. Sherill
Z. phys. Chem. 43, 706 (1903)
/7/ G. Bernhard, O. Hladik
Isotopenpraxis 20, 394 (1984)

A KINETIC STUDY ON THE ROLE OF COMPLEX FORMATION IN THE ION EXCHANGE SEPARATION OF RARE EARTHS BY MEANS OF DTPA

L. Baraniak
Research Center Rossendorf Inc., Institute of Radiochemistry

The influence of complex formation kinetics on the ion exchange rate and its contribution to the theoretical plate height (HETP) has been estimated. For this purpose the migration distance of the undissociated complex in the chromatographic separation process was determined from the mean life of the species (τ) and the mobile phase flow rate (v_m) /1/. In this way H_r equivalents the apparent unability of the chelated ion to interact with the functional groups of the resin. In the case of low reactivity and high flow rates H_r can markedly contribute to HETP.

According to Glentworth et al. /2/ the exchange of the metal ion bound as diethylenetriamine-pentaacetic acid (DTPA) complex is initiated by the protonation of the carboxylic acid groups, i.e. by acid-catalysed dissociation, followed by the rearrangement of the complex, with

$$[CeH(DTPA)]^- + H^+ \rightleftharpoons [CeH_2(DTPA)] \qquad (1)$$

as the rate determining step in acidic media (pH<6) and the rate equation for the total exchange reaction in the case of Ce(III)

$$\frac{dc}{dt} = k_1 [Ce(DTPA)^{2-}] [H^+]^2 + k_2 [Ce(DTPA)^{2-}] [Ce^{3+}] \qquad (2)$$

(k_1=3.68*10^8 l^2/mol^2*min, k_2=2.13 l/mol*min, E_A≙43.5 kJ/mol).

Considering this, H_r can be calculated from

$$H_r = v_m \times \tau = \frac{v_m}{k_1 [H^+]^2} \qquad (3)$$

In the case of H^+ as counter ions the exchange takes place at low pH's under favourable conditions regarding the complex ki-netics. Hence, the contribution of H_r to HETP is negligible (H_r<10^{-3} cm for pH≤3) (Table 1).

For example at pH 2.5 H_r amounts to 2.8*10^{-5} cm, four orders of magnitude below the experimental values (HETP: 0.5 cm at a flow rate of 10 cm/min). Above pH 4 the complex dissociation is delayed to such a degree that H_r contributes with 10 percent and more to HETP (Table 2).
In general, this behaviour is similar to the EDTA system, but the increase of H_r with the pH is stronger in the case of DTPA as the complexant /3/.

Table 1: Reaction kinetic height equivalent in acidic media (pH = 1.75 to 2.75)

pH	1.75	2.00	2.25	2.50	2.75
$[H^+]*10^2/mol*l^{-1}$	1.778	1.000	0.562	0.316	0.177
$k1[H^+]^2*10^{-6}/min^{-1}$	11.45	3.62	1.145	0.362	0.115
$\tau * 10^6/min$	0.087	0.276	0.874	2.762	8.763
$H_r * 10^5/cm$	0.087	0.276	0.874	2.762	8.763

Table 2: Reaction kinetic height equivalent in weakly acidic media (pH = 4.25 to 5.25)

pH	4.25	4.50	4.75	5.00	5.25
$[H^+] * 10^5/mol*l^{-1}$	5.623	3.162	1.778	1.000	0.562
$k_1[H^+]^2/min^{-1}$	114.5	36.20	11.45	3.62	1.145
τ/min	0.009	0.028	0.087	0.276	0.874
H_r/cm	0.087	0.276	0.873	2.762	8.736

References

/1/ U. Brücher, P. Szarvas
Proc. 3rd Analytical Conference, Budapest, Hungary, 1970, p. 27

/2/ P. Glentworth, B. Wiseall
J. inorg. nucl. Chem. 30, 967 (1968)

/3/ L. Baraniak
Report FZR 92-08, 53 (1992)

A KINETIC ANALYSIS OF THE ION EXCHANGE PROCESSES OF TERVALENT RARE-EARTHS-DTPA COMPLEXES

L. Baraniak, H.-J. Engelmann
Research Center Rossendorf Inc., Institute of Radiochemistry

The efficiency of the displacement chromatographic ion exchange separation of rare earths (RE) by means of diethylene-tetramine-pentaacetic acid (DTPA) has been determined from the analysis of the breakthrough curves and the binary overlapping region according to Spedding and Powell /1/. From the experimentally determined dependencies of the theoretical plate height (HETP) from the flow rate (v_m), the temperature (ϑ) and the resin par-ticle size (d_p) (Eqs. 1-4) conclusions can be drawn concerning the rate determining steps and the contribution of the diffusion in the film and particle as well as the chemical reactions in-volved in the coupled ion exchange and complex equilibria, by means of

$$H = 8.96\times10^{-3} \times v_m + 0.04 \qquad (27\text{-}\mu m\ resin) \qquad (1)$$

$$H = 41.3\times10^{-3} \times v_m + 0.06 \qquad (58\text{-}\mu m\ resin) \qquad (2)$$

$$H = 190\times10^{-3} \times v_m + 0.09 \qquad (125\text{-}\mu m\ resin) \qquad (3)$$

$$\log H = -1.343\times10^{-2} \times \vartheta + 0.908 \qquad (58\text{-}\mu m\ resin) \qquad (4)$$

The evaluation was undertaken on the basis of the "linear-driving-force relations" /2/ supposing the actual reaction velocity to be proportional to the deviation from the equilibrium, e.g.

$$\frac{dx_i}{dt} = k_f(c_i - c_i^*), \qquad k_f = \frac{3D_f}{(\delta \times d_p)} \qquad film\ diffusion \qquad (5)$$

$$\frac{dx_i}{dt} = k_p(x_i - x_i^*), \qquad k_p = \frac{56D_p}{d_p^2} \qquad particle\ diffusion \qquad (6)$$

(x_i/c_i - species concentration in the resin/in the solution, D - diffusion coefficient, δ - film thickness, * equilibrium)

with the HETP resulting from the ratio of the band migration (v_b) to the velocity constant ($k_{f,p}$).

Table 1: Film-diffusion-caused height equivalent

d_p/µm	27	58	125
$\delta*10^3$/cm	1.16	1.28	1.43
H_f/cm, calc.	$0.165*10^{-3}$	$0.337*10^{-3}$	$0.942*10^{-3}$
$(H-H_0)$/cm, exp.[a)]	0.095	0.428	1.95

[a)]DTPA: 0.025 m, pH = 8; v_m = 10 cm/min; ϑ = 95 °C; v_b = 0.431 cm/min

- Effect of Film Diffusion

The contribution of film diffusion to the HETP has been calcu-lated by means of $D_f = 0.775*10^{-5}$ cm²/s (20 °C), E_A = 25 kJ/mol /3/ and $\delta = 0.05*d_p*Re^{-0.84}$ /4/ with the result of H_f values to be three orders of magnitude below the experimental ones (Table 1). Therefore, film diffusion represents a fast step in the reaction series, which does not control the exchange of the tervalent RE-DTPA complexes on fine-grained resins at elevated temperatures.

Table 2: Particle-diffusion-caused height equivalent (H_p/cm) in dependence on the flow rate

d_p [µm]	27		58		125	
v_m [cm/min]	H_p	$H-H_0$[a)]	H_p	$H-H_0$	H_p	$H-H_0$
5	0.045	0.040	0.208	0.190	0.965	0.920
10	0.090	0.083	0.415	0.383	1.93	1.85
15	0.135	0.128	0.623	0.605	2.89	2.80
20	0.180	0.166	0.836	0.855	3.86	
30	0.270	0.259	1.246	1.186		
40	0.316	0.338	1.667	1.562		

[a)]DTPA: 0.025 m, pH = 8; ϑ = 95 °C

- Effect of Particle Diffusion

Applying $D_p = 0.112*10^{-8}$ cm²/s and $E_A = 30$ kJ/mol /5/ the computed H_p-values are in a good accordance with the experimental data regarding both the dependence on the flowrate at different particle sizes (Table 2) and the temperature function (Table 3).
The comparison with the plate heights caused by the film diffusion and the chemical reaction /6/ provides evidence for the particle diffusion to be the rate controlling step in the ion exchange process in question. From this, a further im-provement of the separation can be predicted in the case that the diffusion hindrance in the resin particle would be reduced.

Table 3: Particle-diffusion-caused height equivalent (H_p) in dependence on the temperature

ϑ [°C]	D_p*10^8 [cm²/s]	H_p [cm] calculated	$H - H_0$ [cm][a] experimental
20	0.112	4.82	4.36
35	0.201	2.69	2.74
50	0.342	1.58	1.73
65	0.556	0.972	1.09
80	0.876	0.623	0.684
95	1.30	0.416	0.428

[a]DTPA: 0.025 m, pH = 8; d_p= 58 µm; v_m= 10 cm/min

References

/1/ F.H. Spedding, E. Powell
J. Amer. Chem. Soc. 77, 6125 (1955)
/2/ F. Helfferich
Angew. Chem., Intern. Edn. 1, 440 (1968)
/3/ A.V. Shalinets
Radiokhimiya 14, 269 (1972)
/4/ E.R. Gilliland, R.F. Baddour
Ind. Engng. Chem. 45, 330 (1953)
/5/ G.E. Boyd, B.A. Soldano
J. Amer. Chem. Soc. 75, 6091 (1954)
/6/ L. Baraniak
this report, p.12

ION EXCHANGE SEPARATION OF TRACE AMOUNTS ADJACENT RARE EARTHS FROM GADOLINIUM BY MEANS OF NITRILOTRIACETIC ACID

L. Baraniak, H.-J. Engelmann
Research Center Rossendorf Inc., Institute of Radiochemistry

The preparation of high purity Rare Earths (RE) requires the removal of neighbouring RE impurities to a level below 10 ppm. Starting with an analytical grade product (≥99.9%) that means RE impurities have to be reduced at least by a factor of 100 (from 10^3 to <10 ppm).

Owing to the close resemblance of the elements in the RE series the separation of trace amounts from a main component can only be achieved by efficient processes capable of generating a great number of separation stages, for example, by High Performance Ion Exchange Chromatography.

Investigations on the behaviour of minute RE traces (^{144}Ce, ^{147}Nd, ^{153}Sm, $^{154/155}$Eu, ^{90}Y, ^{160}Tb, ^{159}Dy) in Gadolinium during the displacement chromatographic ion exchange process by means of nitrilotri-acetic acid (NTA) as the complexant revealed that most of the impurities have been separated from the main amount of Gd and enriched in the front as well as the rear edge of the band (Fig.1).

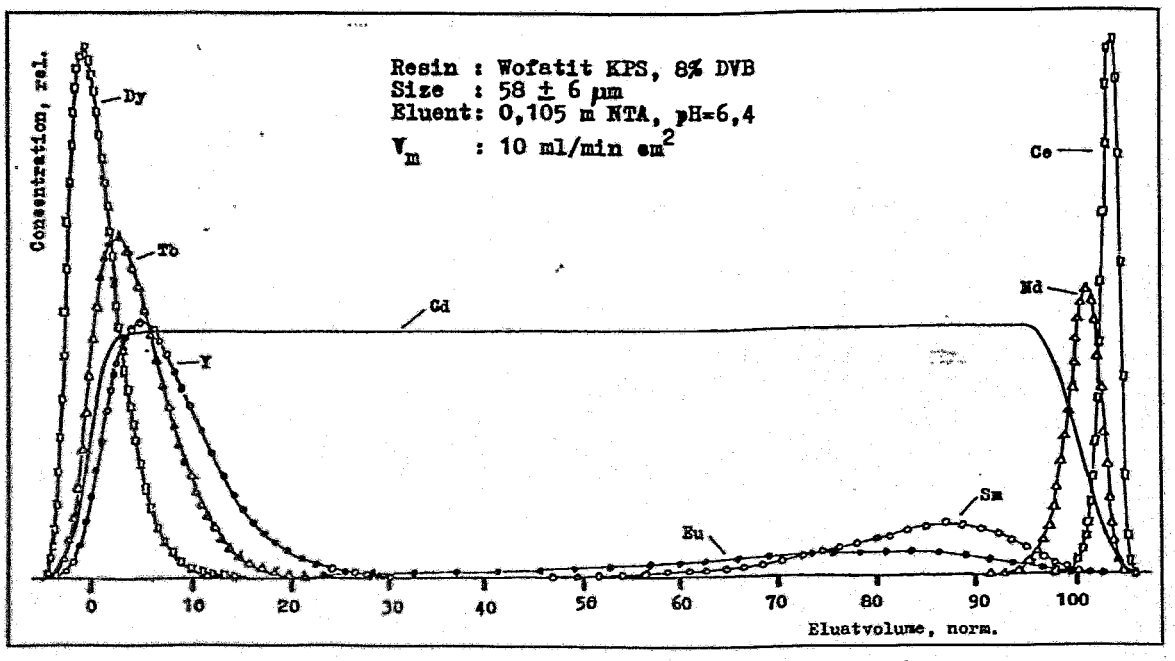

Fig. 1: Displacement chromatographic ion exchange purification of Gadolinium by means of a polystyrene sulfonic acid resin and NTA as complexant

The concentration of the traces appears to follow a logarithmic normal distribution with the mean value (μ) and the standard deviation (σ) being fairly well determined by the efficiency parameters (HETP, sepatation factor) according to the separa-tions by means of DTPA. This includes also the correlation with
the separation conditions via the dependence of HETP on the resin particle size, the eluent flowrate and the temperature/1/.

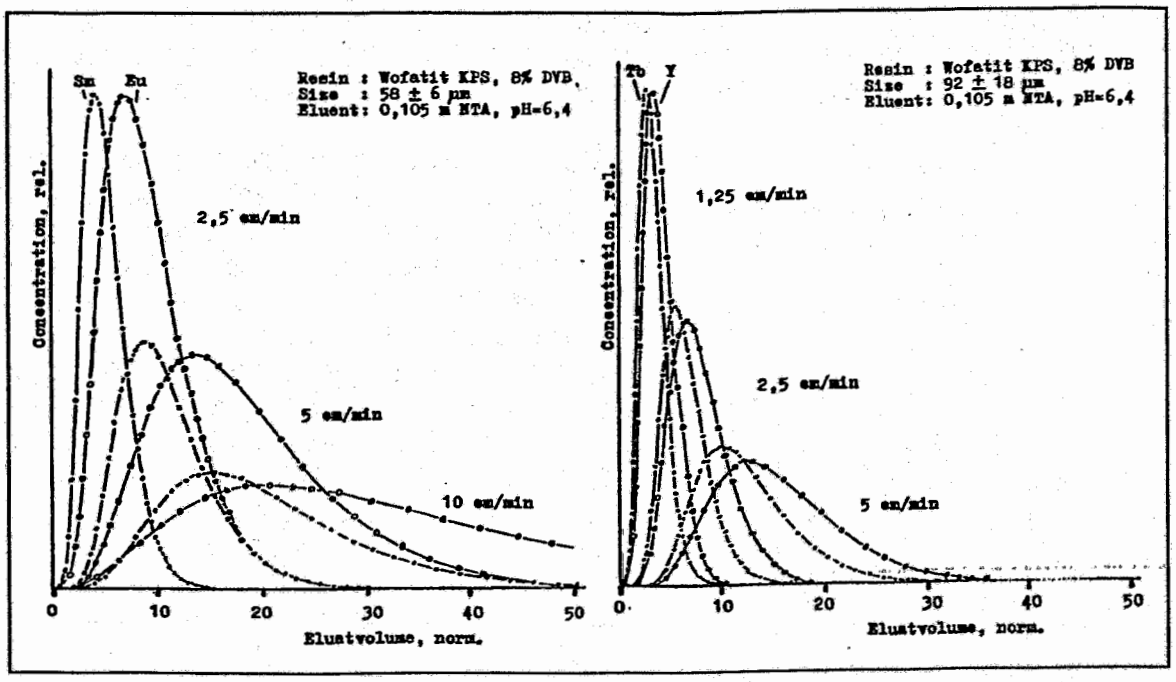

Fig. 2: Distribution of Sm, Eu and Tb, Y in dependence on the flowrate using fine-grained (left) and medium-sized resin (right)

Thus, for instance, a good separation of the heavier and the lighter RE from Gd, with the exception of Sm and Eu, can be achieved at relatively high flow rates by means of a small-particle resin (Fig. 1). In the case that Sm and Eu have to be removed, the separation must be carried out at considerably reduced eluent flow rates (< 5 ml/min) (Fig. 2, left). Coarser particles deteriorate the separation. Using a medium-sized resin Sm and Eu can not be separated from the Gd and the removal of Tb and Y is only successful at low flow velocities too (Fig. 2, right).

References

/1/ L. Baraniak
Report FZR 92-08, 59 (1992)

STEADY STATE OXYGEN ACTIVITIES AT SILVER SURFACES IN REACTING OXYGEN-HYDROGEN MIXTURES

D. Rettig
Research Center Rossendorf Inc., Institute of Radiochemistry

Silver aerosols with gas mixtures of hydrogen, water vapour, oxygen and volatile fission products (iodine and tellurium and their compounds) can be formed in the late stages of a severe light water reactor core degradation accident /1/. The adsorption of the fission products onto silver decisively depends on the local oxygen coverage or chemical oxygen activity at the outer surface under the reactive non-equilibrium conditions.

In the following, an example of the in-situ measurement of the steady state oxygen potential at silver surfaces in reactive oxygen-hydrogen-nitrogen mixtures will be given. Thereafter, the effects will be discussed by simple kinetic considerations.
The basis for the measuring method is a high-temperature solid electroyte potentiometric cell (according to the principle of the so-called lambda automative exhaust gas probe, but working at a lower temperature, 400°C). Vapour deposits of silver were made the electrodes of the galvanic cell at both sides of a stabilized zirconia tube. A cross section of the tube wall is depicted schematically in Fig. 1.

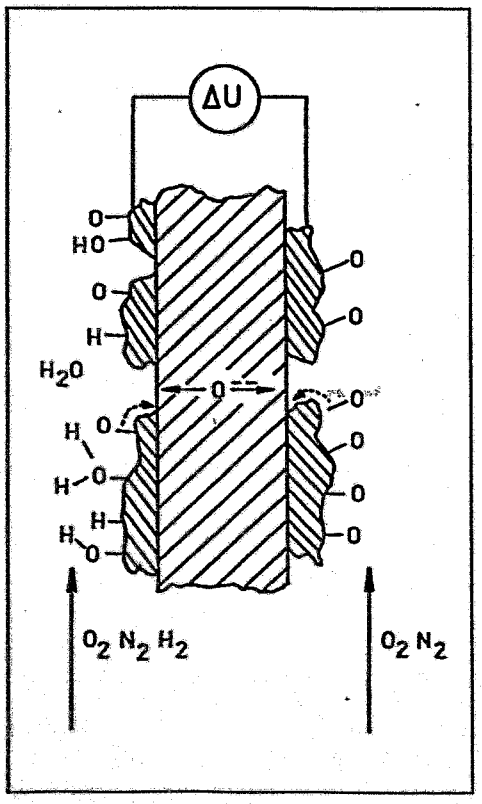

Fig. 1: Cross-section of a solid electrolyte tube wall with oxygen ion conductivity (O^-) and with porous layers of vapour deposited silver at both sides

The right electrode (the reference side R) was streamed around with clean air (N_2+21%O_2), whereas the air at the left electrode (the measuring side M) contained also up to 2000Vol.ppm hydrogen. Fig. 2 shows the response of the voltage (ΔU) of the electrochemical cell to the gas flow rate with different hydrogen contents at 400°C. In Fig. 3 the concentration dependencies of the voltage on the hydrogen concentrations at different flow rates are given.

To provide the basis for understanding the high voltage differences measured (>100mV) it should be mentioned that for equilibrium conditions (that means, for complete burning of the hydrogen in the excess of oxygen) the voltage should be as low as -0,07mV even for the highest content of hydrogen (2000Vol.ppm), according

to the NERNST equation

$$\Delta U = \frac{RT}{4F} \ln \frac{p_{O_2}{}^{M}}{p_{O_2}{}^{R}} \qquad (1)$$

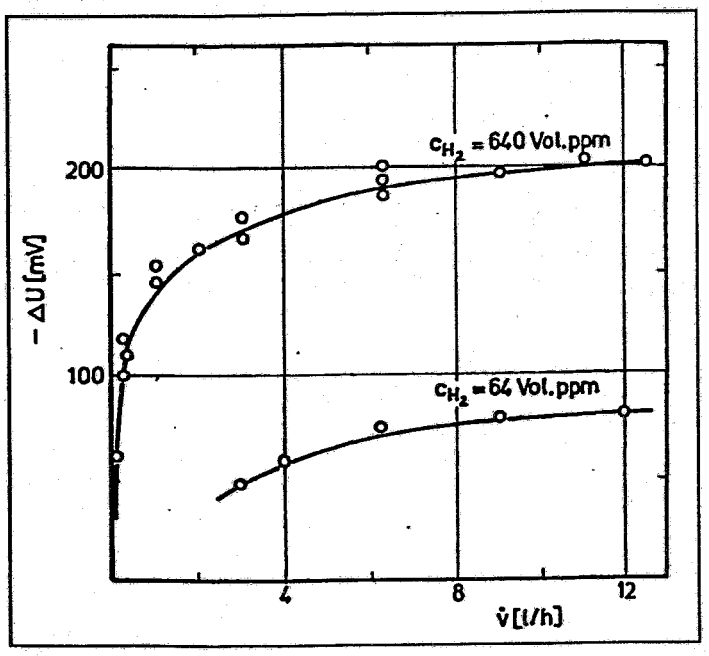

Fig. 2: Response of the voltage to the flow rate of air-hydrogen mixtures at different hydrogen concentrations at 400 °C (cross section of the flow: 0,63 cm²)

Fig.2 shows that the voltages tend to approach these low values at very low flow rates (high retention times to equilibrate) of the gas mixtures. But at flow rates higher than 12l/h (= 5,3cm/s) the steady state voltages are found to be inde-pendent of the gas flows. A surface reaction of hydrogen with oxygen is assumed to determine this steady state.

It was C. Wagner /2/, who suggested that in flowing reacting gases, the voltage should be interpreted as a response to the dissociatively adsorbed atomic oxygen species, which are to be found as intermediates in heterogeneous surface reactions. This principal idea will be the basis for the following crude and schematic consideration of the effects. Among the gas phase and precursor processes of the sequences of the consecutive reactions the probable rate determining steps are considered only.

These are:

$$O_2 \xrightarrow{k_2} 2\,O_{(ad)} \qquad (2)$$

1. The dissociative oxygen adsorption at the silver surface.

2. The reaction of the dissociatively adsorbed oxygen with hydrogen in a LANGMUIR-HINSHELWOOD or in an ELEY-RIDEAL reaction.

$$H_2 + O_{(ad)} \xrightarrow{k_3} H_2O \qquad (3)$$

A clear-cut destination of the two reaction mechanisms is not necessary for this consideration.

Further, the following simplifications and assumptions are made:

3. Competetive and cooperative adsorption processes are not considered and the relative oxygen coverage is expressed by the ratio of the steady state activity (a*) of the atomic oxygen to that of the equilibrium activity (a). That meanste adsorption isotherm is approximated by a linear activity-coverage expression in the region under discussion.

4. The electrochemical exchange reaction of the oxygen adsorbed in steady-state with the electrolyte runs reversibly at the electrode

$$O_{(ad)} + 2\,e^{--} \rightleftharpoons O^{--} \qquad (4)$$

thus building up the voltage ΔU of the probe. Thereby the adsorbed oxygen can move by surface migration to the three phase lines of the gas-solid/electrolyte-metal contact (Fig. 1, see the dash-lined arrows).

5. According to TAKAISHI /3/ the steady state oxygen activity (a*) (and also the equilibrium activity (a) of oxygen) is standardized via

$$(a^*)^2 \equiv p_{O_2}^* = p_{O_2}^M \qquad (5)$$

under equilibrium conditions of reaction (2). The term $p_{O_2}^*$ can be read as the virtual oxygen pressure being in equilibrium with the steady state surface activity (a^*).

IMRE /4/ determined the typical rate laws for the oxygen adsorption at silver surfaces (6) and for the reaction of a burnable gas with O(ad) (7) and found the following velocities of the reactions (2) and (3).

$$v_2 = k_2\, p_{O_2}^{\frac{1}{2}} \left[1 - \left(\frac{a^*}{a} \right)^2 \right] \qquad (6)$$

$$v_3 = k_3 \left(\frac{a^*}{a} \right) p_{H_2} \qquad (7)$$

Under steady state conditions ($2v_2=v_3$) the ratio of the steady state surface oxygen activity (a*) to the equilibrium oxygen activity (a) can be calculated from (6) and (7):

$$\left(\frac{a^*}{a} \right) = \sqrt{\left(\frac{k_3 \, p_{H_2}}{4 \, k_2 \, p_{O_2}^{\frac{1}{2}}} \right)^2 + 1} - \frac{k_3 \, p_{H_2}}{4 \, k_2 \, p_{O_2}^{\frac{1}{2}}} \qquad (8)$$

Insertion of the relative oxygen activity from (8) into the NERNST equation resulting from (1) and (5)

$$\Delta U = \frac{RT}{2F} \ln \frac{a^*}{a} \qquad (9)$$

yields calculated values for the steady state voltages in the reactive gas at the measuring electrode.

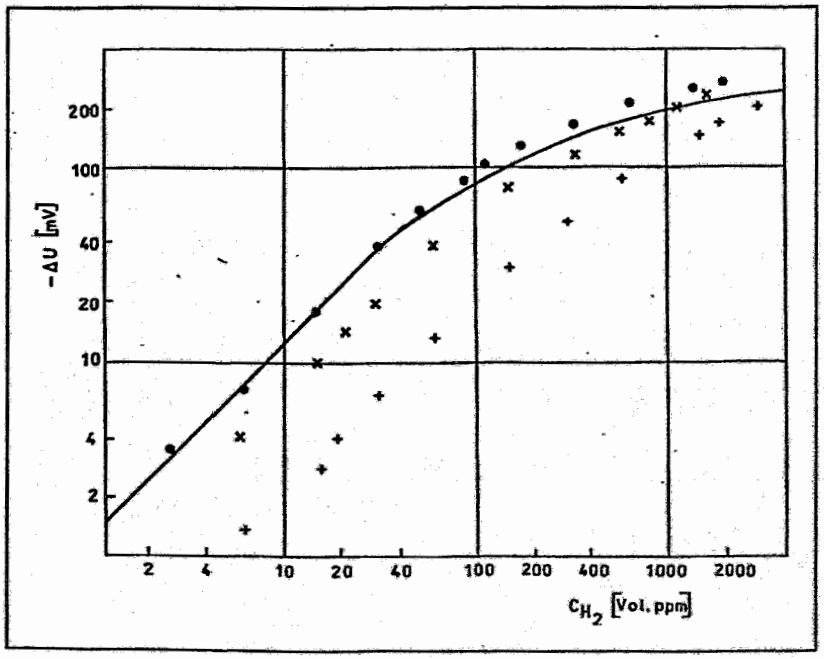

Fig. 3: Dependencies of the voltage on the hydrogen concentrations at 400°C

++ flow rate = 0,3l/h (=0,13cm/s)
xx flow rate = 3l/h (=1,33cm/s)
oo flow rate = 12l/h (=5,31cm/s)
— calculated curve, equation (8) and (9) with $k_3/k_2 = 79700 atm^{-1/2}$

Fig.3 presents the calculated curve using the ratio of the rate constants $k_3/k_2 = 79700 atm^{-½}$ which was determined from a fitting of the linear branch of the curve /5/. The agreement of the shape of the curvature with the measured values is relatively good taking into account the high degree of simplification involved. The results point out that at silver surfaces in flowing air the oxygen activity or the virtual oxygen pressure is considerably reduced by traces of hydrogen. Table 1 shows that the oxygen activity was 5 decades and the virtual oxygen pressure was 10 decades

lower than the equilibrium air values after introducing 0,1Vol%H_2. Thus, species to be adsorbed (such as Iodine and Tellurium and their compounds) will encounter nearly reducing conditions at silver surfaces even in a high excess of oxygen in the gas. This is because the dissociative oxygen adsorption is a relative slow process compared to the fast reaction of the adsorbed oxygen with traces of hydrogen.

Table 1:

From the experimental voltages (Fig. 2) calculated steady state virtual oxygen partial pressures $p_{O_2}^*$ and oxygen activities (a^*) at silver surfaces in air with H_2 added

H_2, added Vol.ppm	equilibrium p_{O_2}/atm	virtual $p_{O_2}^*$/atm	a^*
0	0,210	0,21	0,46
10	0,210	0,086	0,29
100	0,210	$2{,}12*10^{-4}$	0,015
2000	0,209	$2{,}74*10^{-11}$	$5{,}24*10^{-6}$

References

/1/ B. Bowsher
Progress in Nuclear Energy 20, 199 (1987)

/2/ C. Wagner
Adv. Catal. 21, 323 (1970)

/3/ T. Takaishi
Z. Naturforschg. 11a, 297 (1956)

/4/ I. Imre
Berichte der Bunsengesellschaft 72, 863 (1986)

/5/ D. Rettig
Report ZfK-489, 202 (1982),
Report ZfK-629 (1986)

IN-LINE OXIDATION STUDIES OF METALS

C.Nebelung, D.Rettig
Research Center Rossendorf Inc., Institute of Radiochemistry

1. Introduction

The deposition of aerosol particles or gas-borne noxious materials on surfaces of tubes and their resuspension and revaporization into a flowing gas are of interest in a nuclear reactor accident and in the purification of industrial exhaust gas. Both, deposition and revaporization depend on the surface conditions of the tube, the roughness and the amount of adsorbed, absorbed or chemical bound oxygen / 1,2,3 /. For this reason the investigation of the kinetics of the oxidation at various temperatures and gases is significant.
The solid electrolyte coulometry with a calcia stabilized zirconium-dioxide-tube system is a precise method to determine the oxygen exchange of a sample with a carrier gas stream. By the combination of coulometry and potentiometry the partial pressure of oxygen, hydrogen and water and also the amount of the deposited oxygen on the surface can be determined.

2. Experimental

The sample to be investigated is reduced or oxidized at the temperature T in a He-H_2-H_2O gaseous mixture flowing with a constant rate. The gas is prepared and analyzed in the first CaO-stabilized ZrO_2 solid electrolyte tube (5I) Fig. 1.

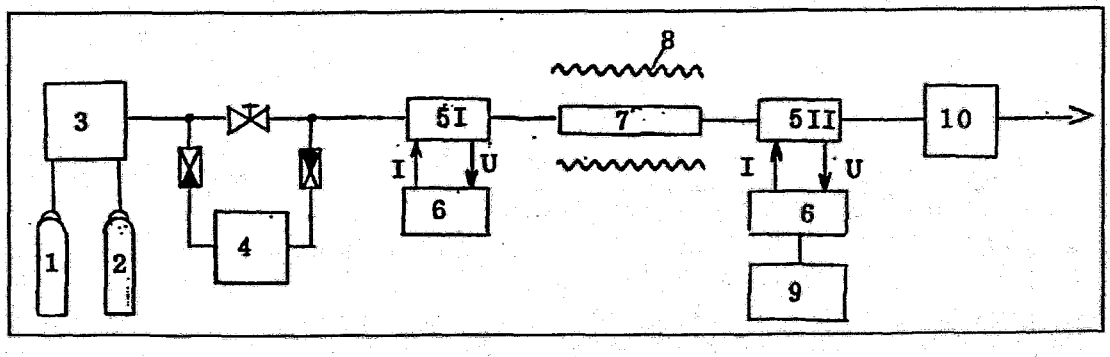

Fig. 1: Measuring principle
I current, U voltage, 1 helium, 2 helium + hydrogen,
3 flow controller, 4 vaporizer, 5 solid electrolyte cell,
6 current control, voltage meter, temperature control,
7 sample, 8 furnace, 9 personal computer,
10 flow meter

This gas with a well-defined oxygen potential (NERNSTs equation) reacts in a furnace (8) with the sample (7). During the reaction the changes of hydrogen concentration in the gas flow are measured continuously by coulometric titration with the second solid electrolyte cell (5II) / 4,5 /. The change of the hydrogen concentration is proportional

to the change of the oxygen concentration. According to FARADAYs law the oxygen exchange is calculated by integration of current-time curves during the reaction. The possible measuring ranges of partial pressures of oxygen, hydrogen and water are between

$p_{O_2} = 3*10^{-22}$ ... 0.2kPa
$p_{H_2} = 10^{-5}$ ... 0.1kPa
$p_{H_2O} = 5*10^{-3}$ ... 20.0kPa

3. Results

In most cases a redox equilibrium between the gas (helium carrier gas with oxygen, water and hydrogen) and the sample was not reached. The oxidation process stopped, when the sample was cooled. An analogous problem, the oxidation of UO_2 (fuel in nuclear reactors) without an equilibrium between sample and gas is described in / 6 /. In this work the oxidation of metals, which are used as reactor materials, is described. The following figures show the oxidation process of iron, nickel, stainless

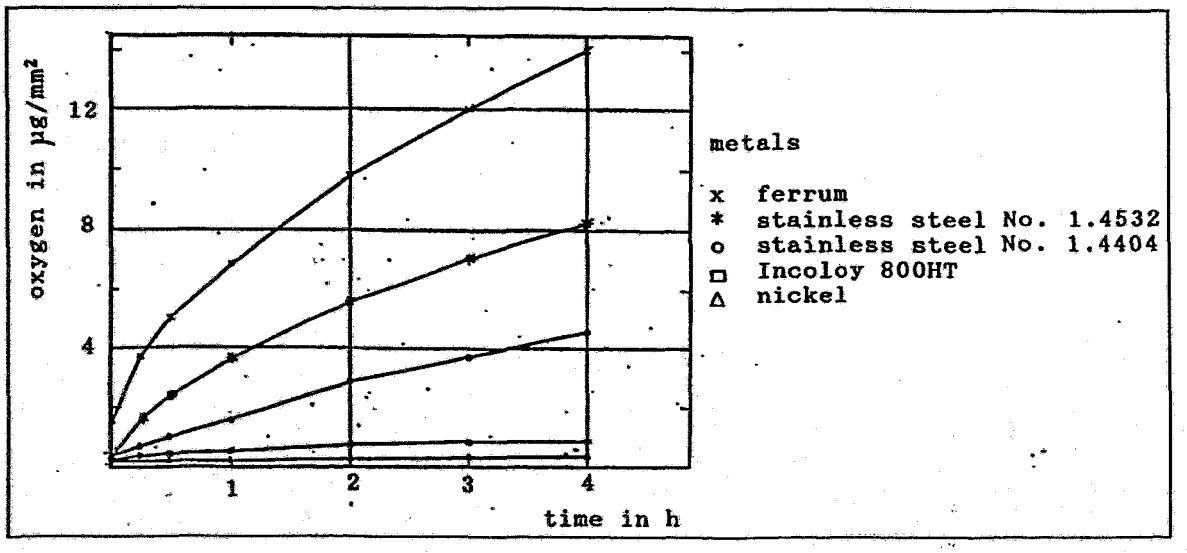

Fig.2: Dependence of the surface oxidation on time at various metals (temperature: 700°C, H_2O/H_2: 488, partial pressure:

steel 1.4404 (AISI 316L) and 1.4532 and INCOLOY 800HT in several helium-water-hydrogen gaseous mixtures at temperatures between 300 and 700°C.

Fig. 2 shows the surface-oxidation versus time curve for several materials at 700°C and a water-hydrogen ratio of 480. After 4 hours for nickel and INCOLOY 800HT the reaction on the surface is nearly finished. In the cases of stainless steel and especially of iron a faster oxidation was observed. From the beginning up to 15 min the oxidation is linearly dependent on time, later it follows a square root function. That means that the oxidation process is not limited in its later stages by the oxygen

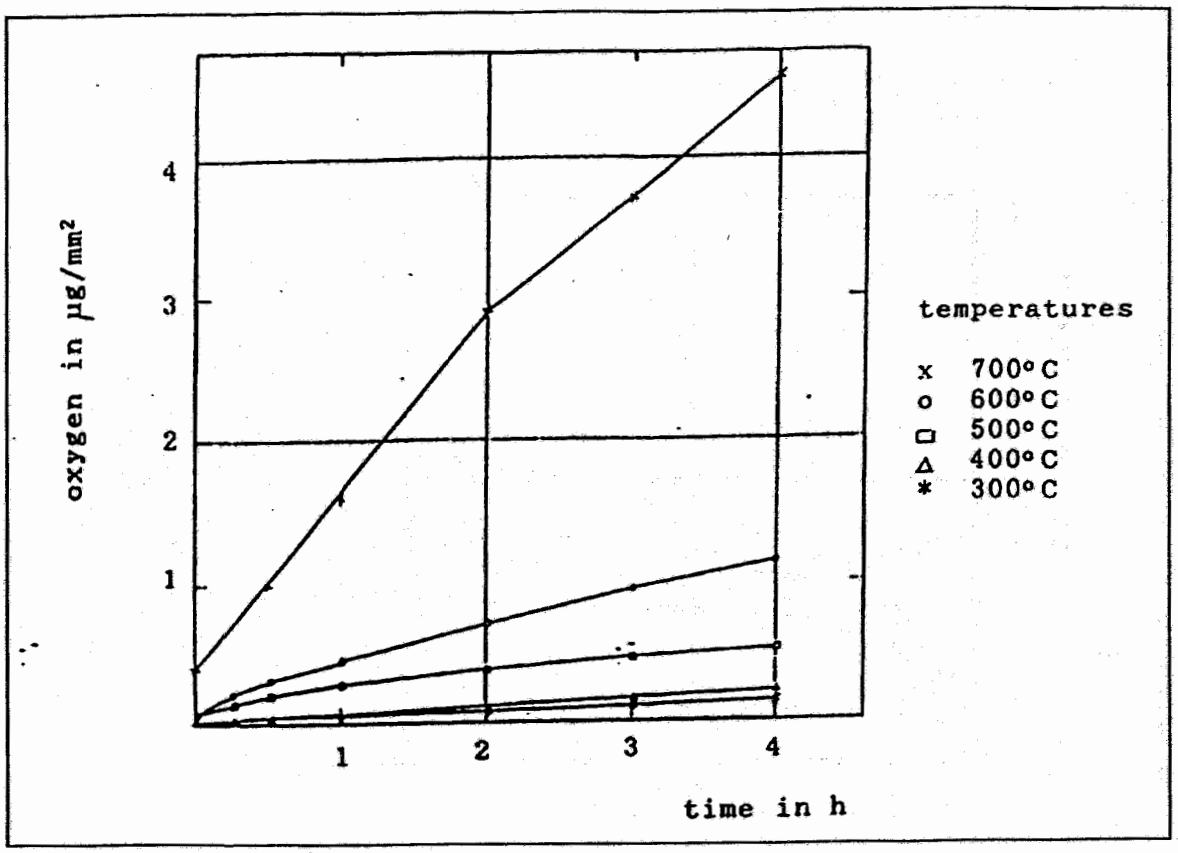

Fig. 3: Dependence of the Surface oxidation on time at various water-hydrgen ratios (Temperature: 700 °C, stainless steel AISI 316L)

transport in the gas to the surface of the metal.

Fig. 3 shows the surface oxidation versus time curve of stainless steel AISI 316L at a water-hydrogen ratio of 480. The oxidation is higher at higher temperatures.

In Fig. 4 the oxidation of the surface of stainless steel No. 1.4404 is described at 700°C at several water-hydrogen ratios. At the ratio 0.15 the oxidation was nearly complete after one hour. The higher the ratio, the thicker is the oxide layer.

There may be several transport and reaction mechanisms to explain this behaviour (water vapour transport in the gas phase, gas-surface interface reaction, diffusion processes in the growing oxide layer and the dependencies of the latter two processes on the local oxygen activities).

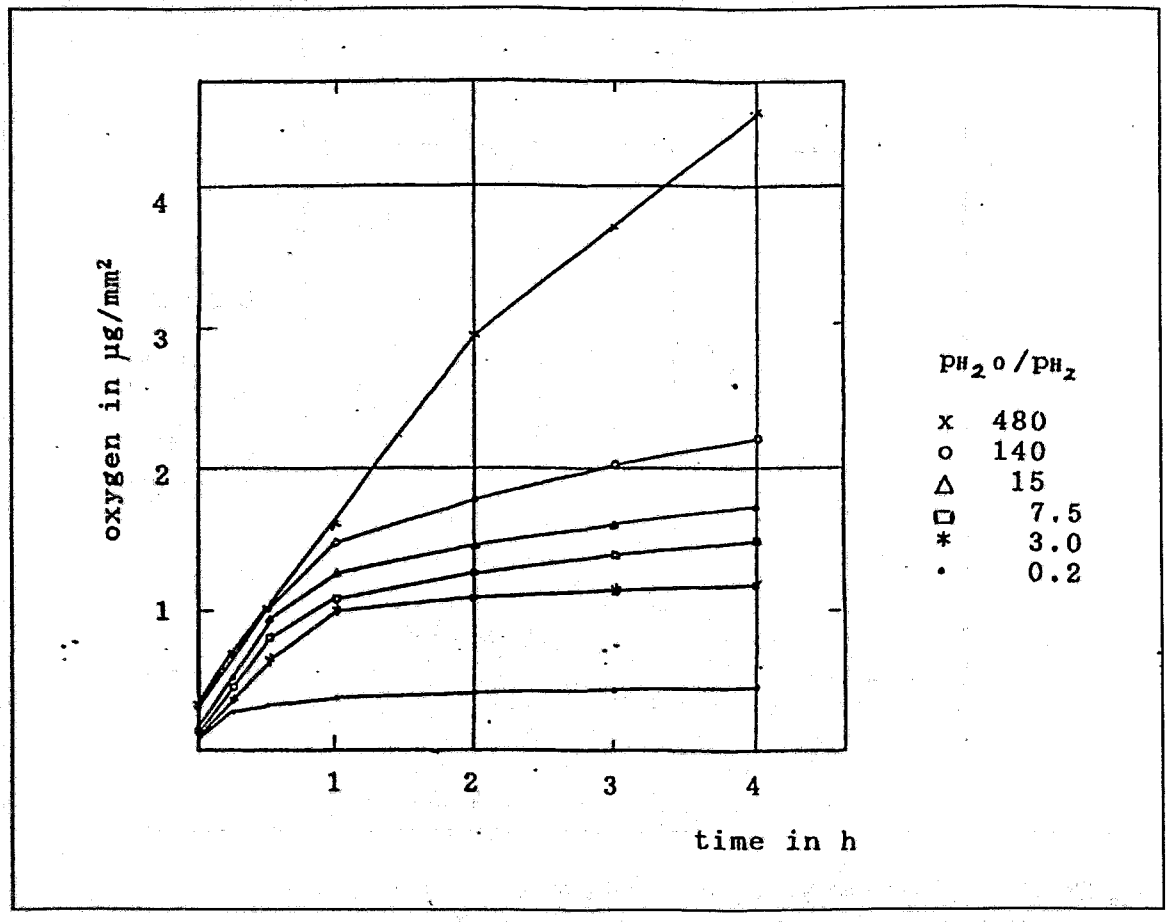

Fig. 4: Dependence of the surface oxidation on time at various water-hydrogen ratios (temperature: 700°C, stainless steel AISI 316L)

4. Conclusion

The solid electrolyte method in a flowing gas stream is a very precise in-line method to determine oxidation-reduction-reaction kinetics of solids. Especially in surface oxidation processes
the accumulation of oxygen can be observed as a function of time. In this study gas mixtures with very low water vapour and hydrogen contents have been used. Further experiments are necessary to find out the rate determining step of the oxidation process at different oxygen potentials. Thus extrapolations to the oxidation kinetics at higher water vapour and hydrogen pressures will be possible. The method described is planned to be used in studies of sorption processes of fission products or poisonous materials on growing oxide layers.

Acknowledgement

These studies were supported by the Bundesminister für Forschung und Technologie of the Federal Republic of Germany under contract BMFT 03 ZFK 2015.

References

/1/ B.R. Bowsher, S. Dickinson, A.L. Nichols
Report AEEW-R 1863 (1990)

/2/ F. Sabathier
AEA RS 5164 (1991)

/3/ S. Dickinson
AEEW R 1699 (1983)

/4/ K. Teske, W. Gläser
Microchimia acta 1, 653 (1975)

/5/ Gerätebeschreibung OXYLYT-Meßgerät zur Analyse von Gasen und Festkörpern, ZfK Rossendorf (1991)

/6/ C. Nebelung,
Report FZR 92-08, 77 (1992)

SPAREX - A NEW EXPERIMENTAL LOOP FOR INVESTIGATING THE TRANSPORT BEHAVIOUR OF RADIOTOXIC AND TOXIC GASBORNE CHEMICAL SPECIES

P. Griepentrog, P. Merker, D. Rettig, H. Stöbel, W. Witke,
H. Zänker
Research Center Rossendorf Inc., Institute of Radiochemistry

The SPAREX (**SP**altprodukt- **A**blagerungs- und **R**emobilisierungs-**EX**periment) loop is being erected within the framework of a project supported by the German Ministry of Resarch and Technology. SPAREX is now shortly before its completion in its original conception according to which it was intended to serve as a means for the investigation of High Temperature Reactor accidents. SPAREX is a technical scale facility by the help of which radioactively tracered fission product simulants can be

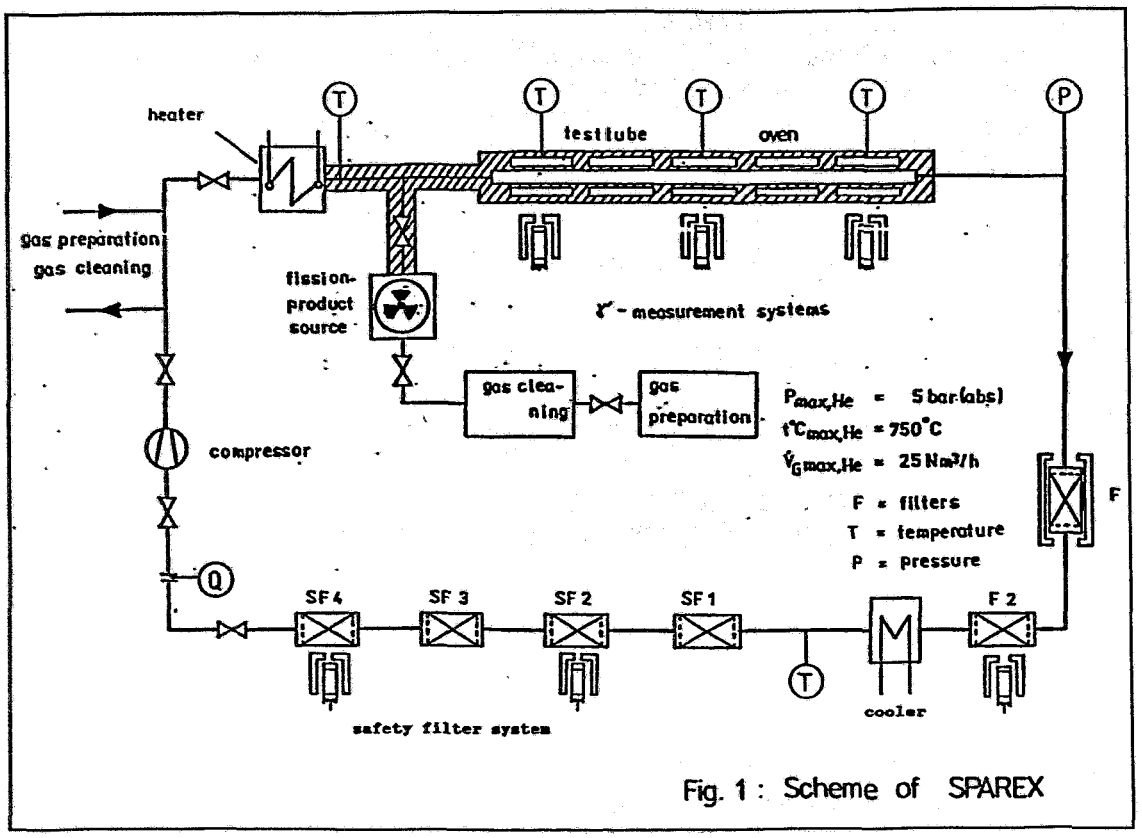

Fig. 1 : Scheme of SPAREX

injected into a helium loop and the deposition as well as remobilisation of these substances in 2 m test tubes can be followed by on-line gamma spectrometry. Figure 1 shows a principal scheme of SPAREX in its original conception.

The principle of the first fission product simulant source, the cesium source, is the evaporation of metallic cesium and its transport as a metal vapour in a slow stream of carrier gas (high pure helium). The cesium metal is exposed to the source sweep gas by cracking a cesium ampoule with the help of a mechanic cracking mechanism after having purged the source branch of SPAREX thoroughly with high-pure helium.

The source strength can be controlled by temperature and/or gas flow regulation. For the first experiments a cesium inventory of about 100 mg tracered by 10 mCi ^{134}Cs is intended to be inserted in the fission product simulant source.

In its original conception SPAREX is not yet suited to investigate processes relevant to severely damaged LWRs. Modifications are necessary to achieve this objective. They are to be completed within the span of time of a year. The most important one is the construction of a facility for humidifying and drying the carrier gas with the help of which relatively high steam concentrations in the test tube atmosphere can be adjusted.

The modified SPAREX loop is to provide the following parameters:

- Test tube inner diameter:	10...20 mm
- Test tube length:	2 m
- Wall temperature of test tube:	200...750 °C
- Pressure (absolute):	0.1...0.4 MPa
- Gas volume flow rate:	0...25 Nm^3/h
- Linear gas flow velocity:	0...60 m/s
- Steam concentration:	0...10 Vol%*
- Hydrogen concentration:	0...4 Vol%

* This refers to the maximum gas volume flow rate; in case of lower flow rates higher values are achievable (reciprocal-linear dependence).

In addition to the humidification and drying of the helium the modifications of SPAREX include the development and fitting of a facility capable of detecting spontaneously formed fission product simulant aerosols. Furthermore the operation with various test tube diameters and materials as well as the insertion of metal sample coupons in the test tube is to be prepared. It is also necessary to develop new fission product simulant sources.

These are

(i) a CsOH source,
(ii) a tellurium source.

After these modifications and completions SPAREX will be a scientific device of relatively wide applicability. It is well suited to carry out investigations into the field of nuclear power plant safety research (assessment of the consequences of hypothetical accidents) but it is not restricted to this application. It can also be used for the investigation of the transport behaviour of other airborne air-polluting toxic substances which tend to show interactions with solids. From a more general point of view the most important features of SPAREX are

- The experiments are performed under the conditions of tube geometry.

- A temperature range of 200 to 750 °C is covered. There is still a great lack of knowledge concerning the chemical transport phenomena in this temperature range since chemical kinetics plays a decisive part.

- A wide range of gas flow velocities is covered.

- A wide range of redox potentials in the tube atmosphere is covered.

- All the ambient conditions in the tube can be adjusted very definitely.

- The deposition and remobilisation phenomena in the test tube can be followed in-situ by radioactive tracering the transported chemical species and on-line gamma spectrometry along the test tube.

An example of the scientific strategy for SPAREX experiments is given in the following paper /1/.

Acknowledgement

These studies were supported by the Bundesminister für Forschung und Technologie of the Federal Republic of Germany under contract BMFT 03 ZFK 2015

References

/1/ H. Funke, et al.
this report, p. 32

THE SCIENTIFIC STRATEGY OF THE SPAREX EXPERIMENTS FOR THE NEXT TWO YEARS

H. Funke, P. Griepentrog, G. Hüttig, P. Merker, D. Rettig,
H. Stöbel, W. Witke, H. Zänker
Research Center Rossendorf Inc., Institute of Radiochemistry

The general possibilities of SPAREX, which are obvious from the preceding article /1/, make this loop a useful scientific tool to investigate the transport behaviour of a variety of chemical species in a relatively wide temperature range under tube geometry conditions as well as to validate and improve codes for the description of this transport behaviour. Thus, SPAREX is also suited to investigate the release and retention behaviour of fission products in the primary system of LWRs under the conditions of core melt accidents which is describable by codes such as TRAPMELT, VICTORIA, RAFT ect.

Comparative calculations with the hitherto existing codes carried out on the same reference problem (as e.g. the PHEBUS-FPT-O problem /2/) show drastic difference in their results. They are caused by certain deficiencies and discrepancies in these codes.

The description of the deposition of CsOH vapour and tellurium vapour onto primary system structural material surfaces in the codes TRAMPELT and VICTORIA may serve as an example of model differences. The deposition rate is given as a first order law in both codes (in VICTORIA only for CsOH):

$$\frac{dm_s}{dt} = - A V_D C_g \qquad (1)$$

m_s = mass on the surface
A = surface area
C_g = concentration in the gas phase
V_D = reaction rate coefficient

In TRAPMELT the reaction rate coefficients are constants having the values of

$V_D = 0.01$ cm s^{-1} for CsOH and
$V_D = 1.0$ cm s^{-1} for tellurium,

which are results of a study by ELRICK et al./3/. According to BOWSHER et al., however, one has to distinguish between two forms of CsOH - a water soluble from and an irreversibly deposited form /4/. VICTORIA takes this differentiation into account /5/. It includes also the temperature dependence of V_D which is assumed to be

$$\ln (10^2 V_D) = \frac{4330}{T} - 7.91 \qquad (2)$$ for soluble CsOH,

$$\ln (10^2 V_D) = \frac{7170}{T} - 2.63 \qquad (3)$$ for insoluble CsOH.

The tellurium deposition is described with the help of an equilibrium model in VICTORIA, not by means of a kinetic law.

Another important feature of VICTORIA, which makes it different from TRAPMELT, is the assumption of a "reaction layer" on the surface in which equilibrium is adjusted and transport processes do not play a role. The thickness of this layer must be fixed by the code user on the basis of external sources of information.

There are further items that are described fairly contradictory in the various codes.

How can SPAREX promote code development?

Because of the on-line gamma spectrometry the fission product simulant deposition in the test tube can be followed in-situ and the kinetic laws of the deposition (first order or different order?) can be determined. The temperature dependence of the reaction rate coefficients can be elucidated by variations of the carrier gas and test tube temperatures. SPAREX can help in finding reasonable "reaction layer thicknesses" for VICTORIA calculations. Thus, the SPAREX experiments can contribute to a better description of the deposition behaviour of certain fission products.

Another field is the investigation of revaporisation processes for deposited species. Deposited fission products can be revaporised from primary system surfaces by increases in temperature due to the radioactive decay heat during a LWR core melt accident. These phenomena, however, need further investigation. SPAREX can contribute to a better understanding of the revaporisation processes. The influence of the redox potential in the test tube atmosphere on the fission product deposition and revaporisation behaviour can be studied with SPAREX. This is another problem which can be modelled only poorly in the calculational codes. Finally, the homogeneous nucleation of fission product aerosols in the temperature and gas flow velocity range covered by the loop can be investigated - a field much under discussion in modelling work currently.

Since the individual SPAREX experiments need to be prepared very thoroughly and since their number per year is limited, these experiments must be based on an elaborate test matrix. It will be worked out in 1993 (in close collaboration with a number of partners outside the Research Center Rossendorf).

Figs. 1 to 4 give first predictions of the cesium behaviour in a SS 304 test tube calculated with the help of VICTORIA.

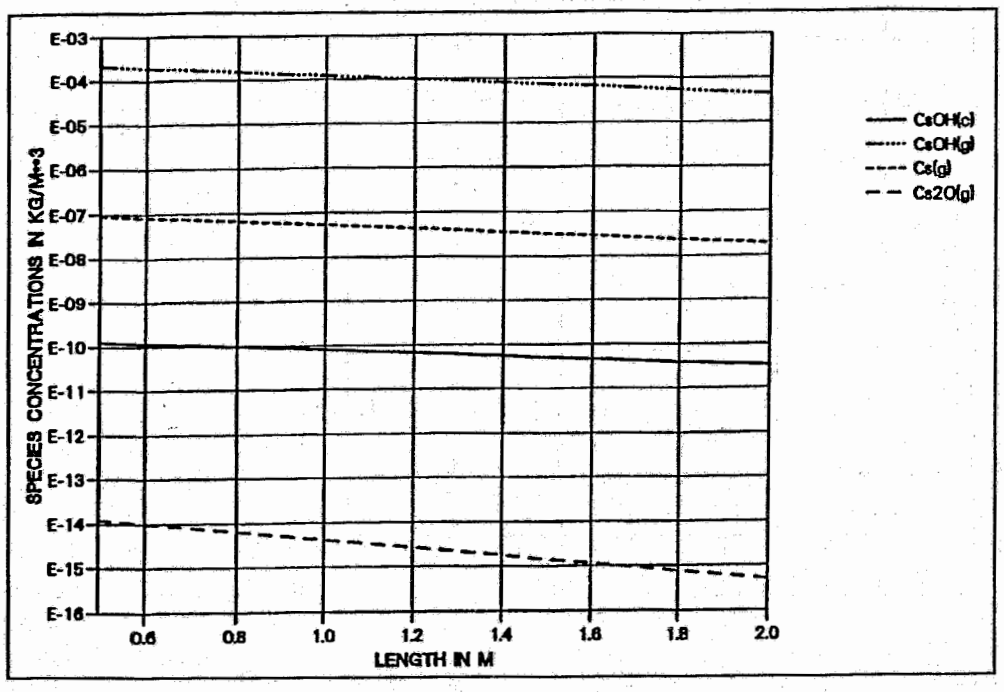

Fig.1: Species concentrations along the tube (923K, 60s)

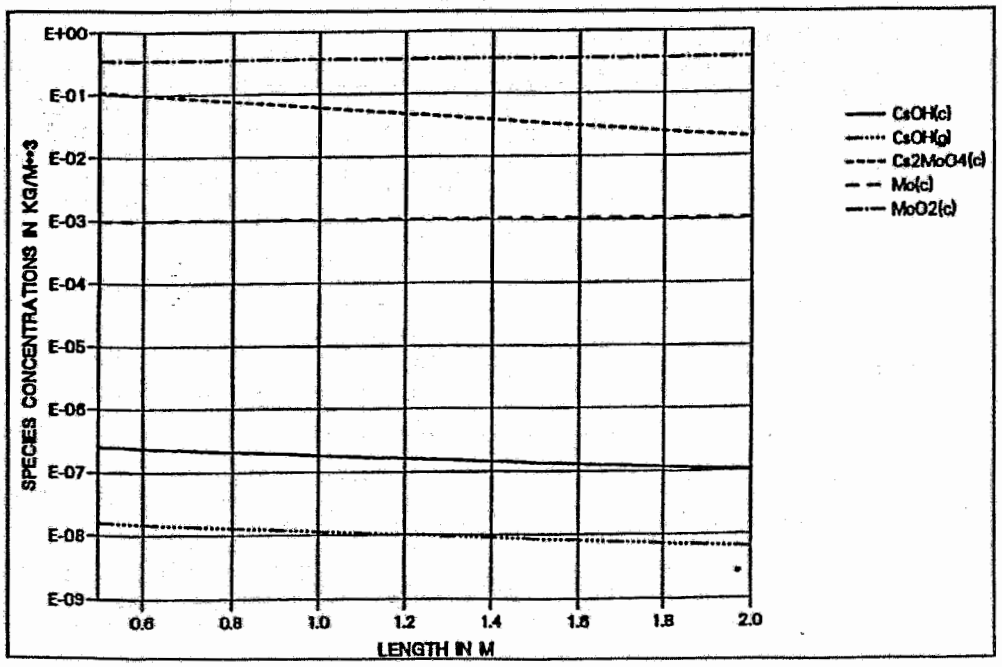

Fig.2: Deposited species concentrations along the tube(923K,60s)

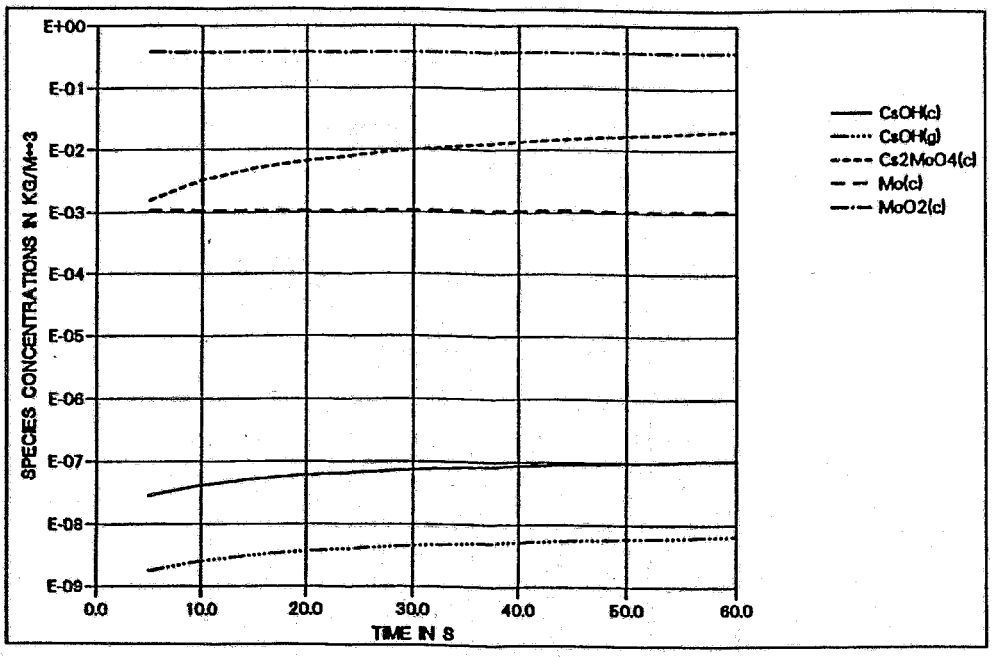

Fig.3: Deposited species concentrations in last cell (923K)

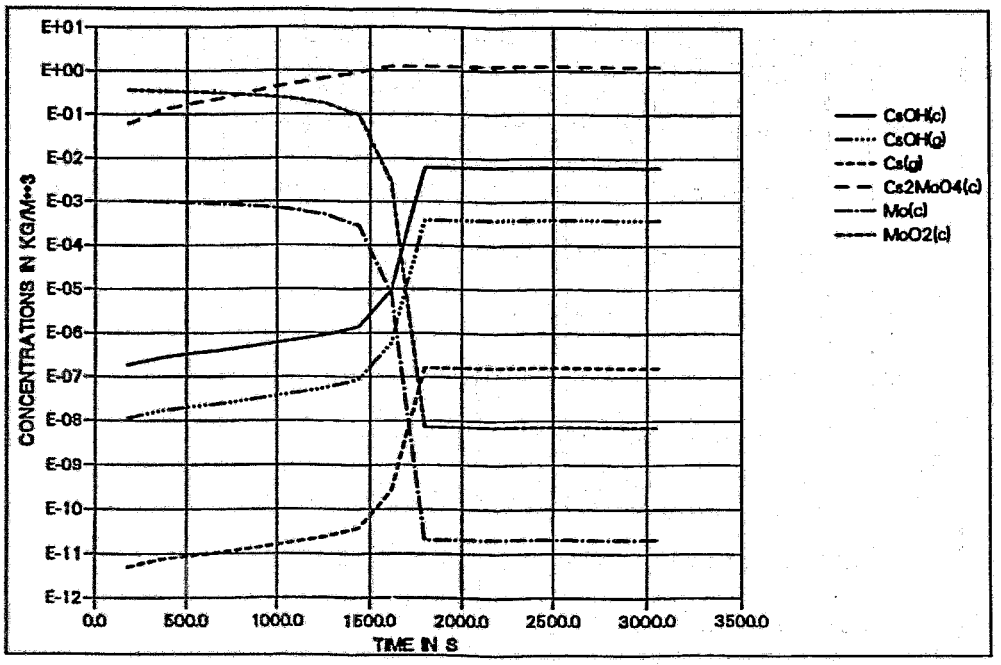

Fig.4: Deposited species concentrations last cell (923K)

The test conditions assumed are

Test tube inner diameter:	12.4 mm
Test tube length:	2 m
Test tube wall temperature:	923 K
Gas temperature in the test tube:	923 K
Pressure:	0.4 MPa (absolute)
Gas flow (linear velocity):	1.6 m/s
Steam concentration:	10 Vol%
Hydrogen concentration:	4 %
Concentration of the FP Simulant:	$3.3*10^{-4}$ kg/m^3

The thickness of the "reaction layer" was assumed to be 0.01 mm. Since in the version of VICTORIA, which was used, the chemical interactions of chromium are not taken into account, chromium was simulated by molybdenum in these first estimations. Chromium has nearly the same chemical parameters (Gibbs energies) as molybdenum and is represented by a compound of the same stoichiometry in the model (Cs_2CrO_4 - Cs_2MoO_4). Fig. 1 shows the gas concentrations of the various cesium species along the test tube, Fig. 2 the concentrations of the deposited species (concentrations within the "reaction layer") and Figs. 3 and 4 the time dependence of the deposited species concentrations at an individual section of the test tube (last cell). The indices c and g stand for "condensed phase" (deposited on the surface or gasborn as aerosols) and "gas phase", respectively.

The Figures are to illustrate the general strategy of research for SPAREX in the field of nuclear power plant safety research which is

a) The prediction of the deposition (and remobilisation) behaviour in the test tube under certain test conditions by the aid of code calculations

b) The SPAREX experiment

c) The comparison between predictions and experimental results; the establishment of hypotheses to explain differences between predictions and experiments

d) Further experiments to confirm or reject these hypotheses

e) The introduction of new insights (new parameters, new theorectical explanations etc.) into the calculational models.

Similar strategies of research are to be developed for the application of the SPAREX loop in other working fields such as the investigation of the transport behaviour of airborne toxic substances in non-nuclear technologies.

References

/1/ P. Griepentrog, et.al.
this report, p. 29

/2/ Report SAWG 92-035/2 (1992)

/3/ R.M. Elrick, et.al.
Report NUREG/CR-3197 / SAND 83-0395, R5 (1984)

/4/ B.R. Bowsher, et.al.
Report AEEW-R 1863 (1984, Revised 1990)

/5/ T.J.Heames, et.al.
Report NUREG/CR-5545, SAND 90-0756, R3, R4, Rev.1 (1992)

2. CHEMISTRY OF HEAVY ELEMENTS

GAS CHROMATOGRAPHIC STUDIES OF MOLYBDENUM OXIDES AND HYDROXIDES

S.Hübener, A.Roß
Research Center Rossendorf Inc., Institute of Radiochemistry

B.Eichler, H.Gäggeler, J.Kovacs
Paul Scherrer Institute, Laboratory for Radiochemistry
Villigen, Switzerland

S.N.Timokhin, A.B.Yakushev
Joint Institute for Nuclear Research, Flerov Laboratory of Nuclear Reactions, Dubna, Russia

In continuation of gas chromatographic studies of oxides and hydroxides of the lighter homologues of element 106 we have studied by thermochromatography the behaviour of molybdenum in quartz columns using a mixture of Ar, O_2 and H_2O as a carrier gas and the uranium fission products ^{99}Mo and ^{101}Mo as indicatory isotopes.
Among others the fission products under study were produced in a thin ^{235}U target installed at the swimming pool reactor SAPHIR of the Paul Scherrer Institut Villigen and transported continuously into the gas chromatography columns over a distance of 130 m by means of the SAPHIR gas-jet system /1/. MoO_3 was used as a cluster material for the gas-jet. To achieve high volatilization yields of Mo under conditions for a complete retention of the aerosol particles on a hot filter the preheating section was longer than in our earlier experiments with W /2/. Besides quartz wool being used commonly as a hot filter material for the retention of aerosol particles we tested quartz capillaries with inner diameters ranging from 0.05 to 0.18 mm.
Fig.1 shows the experimental set-up and a thermochromatogram of an experiment with humid oxygen admixtures to the carrier gas. The thermochromatograms were evaluated from γ-spectrometric off-line measurements of 5 cm sections. With a quartz wool plug as a hot filter as well as with a 6cm long bundle of quartz capillaries a complete retention of aerosol particles was observed as indicated by the complete deposition of ^{91}Sr in the preheating section and on the hot filter and by the activity collected on the glass fibre filter at the end of the column, which was free of radionuclides transported with an oxygen containing carrier gas at temperatures lower than 350 K only in case if attached to aerosol particles.
In a carrier gas containing dry oxygen molybdenum was deposited almost in the same position as ^{91}Sr, most likely as MoO_3 by desublimation:

$$MoO_{3(g)} \rightleftarrows MoO_{3(des)} \qquad (1)$$

As depicted in Fig.1, with humid oxygen admixtures to the carrier gas molybdenum was volatilized completely and transported down to about 400 K. The deposition in a wide temperature range with a maximum at 870 +/- 50 K may be explained with a transport
reaction like :

$$H_2MoO_{4(g)} \rightleftarrows MoO_{3(des)} + H_2O_{(g)} \qquad (2)$$

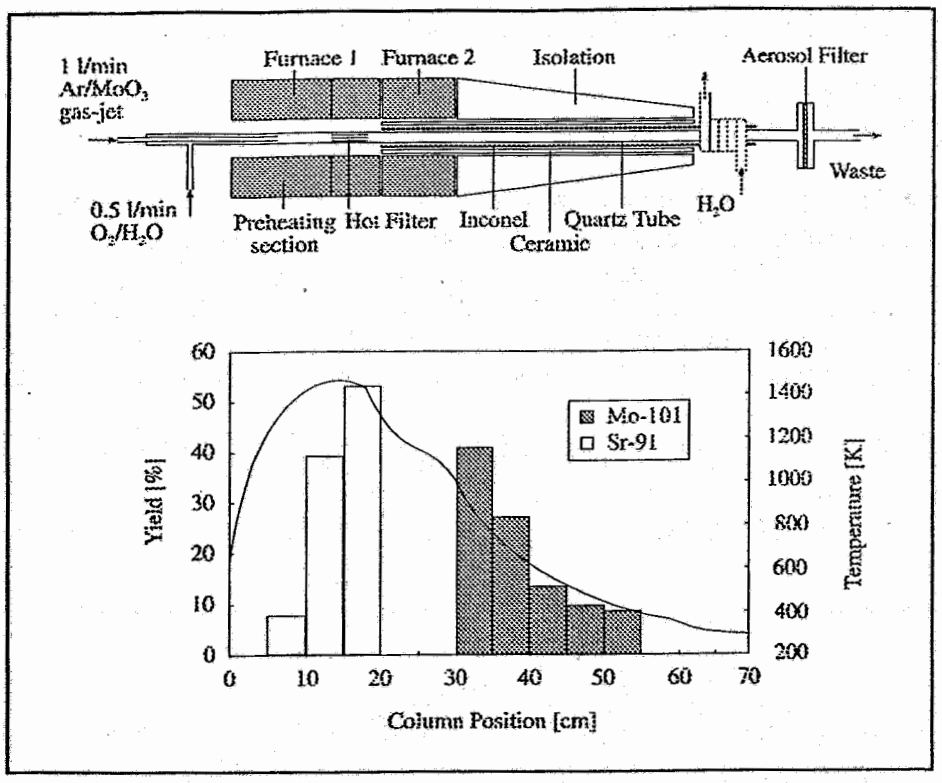

Fig.1: Experimental set-up and distribution of ^{91}Sr and ^{101}Mo

and a desublimation of H_2MoO_4 in the low-temperature region.
To evaluate thermodynamic functions from the experimental data a formalism was used which was published recently for complex transport reactions of iridium oxides and hydroxides in a temperature gradient tube /3/. The resulting adsorption enthalpies were $_{\Delta}H°_{des}$ = -448 kJ/mol for reaction (1) and $_{\Delta}H°_{diss,des}$ = -147 kJ/mol for reaction (2). 0.2 s, the estimated time required to transport Mo with humid oxygen trough the hot part of the column, should be short enough to get high volatilization yields of short-lived isotopes, too. However, this has to be verified experimentally.

Acknowledgement

These studies were supported by the Bundesminister für Forschung und Technologie of the Federal Republic of Germany under contract 06 DR 101 D.

References

/1/ Ya Nai-Qi, D.T.Jost, U.Baltensperger, H.W.Gäggeler
Radiochim. Acta 47, 1 (1989)
/2/ S.Hübener, et al.
Report FZR 92-08, p.71
/3/ B.Eichler, et al.
Radiochim. Acta, in press

SEPARATION OF CARRIER-"FREE" MOLYBDENUM FROM ZIRCONIUM

A. Roß, S. Hübener
Research Center Rossendorf Inc., Institute of Radiochemistry

In preparation for gaschemical studies of carrier-"free" molybdenum as oxide or hydroxide the separation of molybdenum from zirconium was examined.
To obtain carrier-"free" molybdenum a stack of five zirconium foils (< 10 ppm Mo), 20 µm thick each, was bombarded at the 1.20 m cyclotron of the Forschungszentrum Rossendorf for 60 min with 1 µA beams of 27 MeV α-particles. By this ^{93m}Mo ($t_{1/2}$ = 6.9 h) as well as ^{99}Mo ($t_{1/2}$ = 65.9 h) were produced in (α,xn)-reactions.

The distribution of the activity was determined by γ-spectrometry and is shown in Fig. 1.

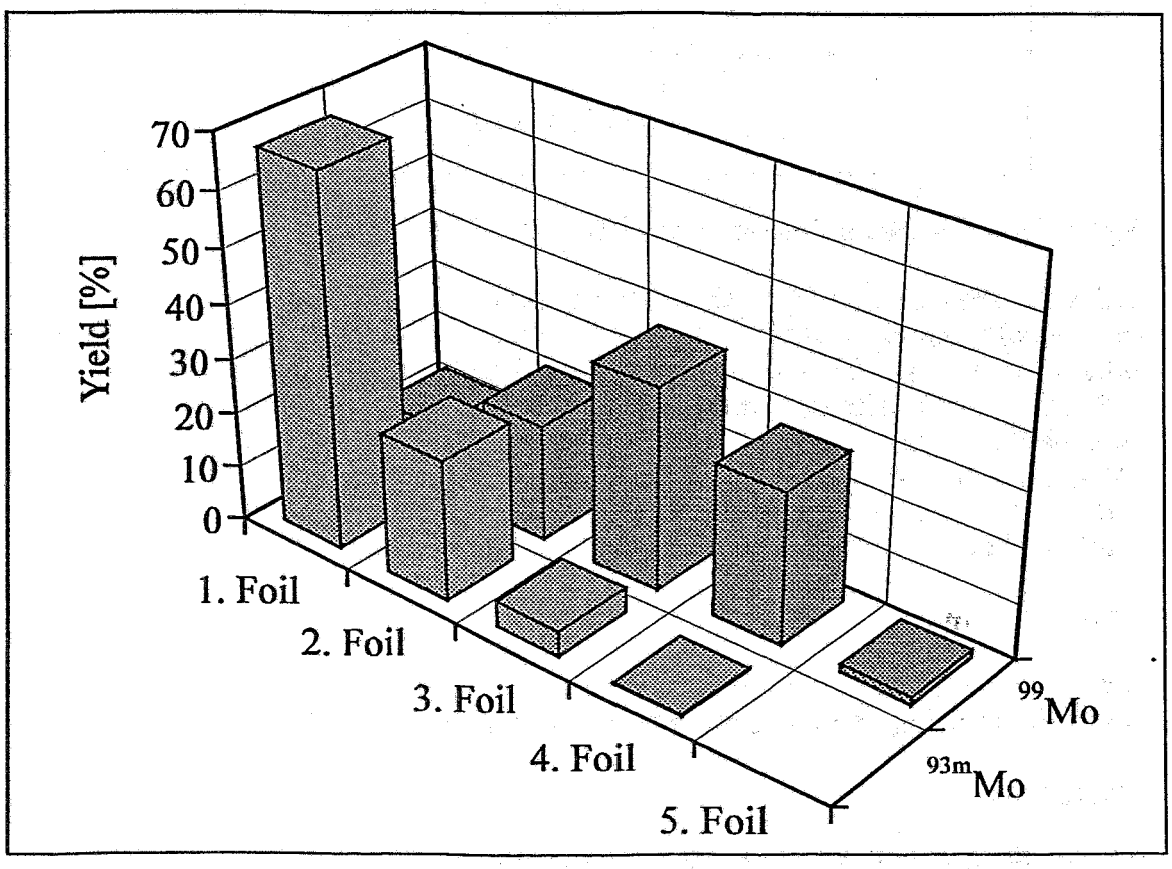

Fig. 1: Distribution of the molybdenum activity in the zirconium foils

As known from literature in dry or moist air, respectively, the following reactions can be observed:

$$2\,Mo + 3\,O_2 \rightleftharpoons 2\,MoO_3 \quad (1)$$

$$Mo + 3\,H_2O \rightleftharpoons MoO_3 + 3\,H_2 \quad (2)$$

$$Mo + 4\,H_2O \rightleftharpoons MoO_2(OH)_2 + 3\,H_2 \quad (3)$$

$$MoO_3 + H_2O \rightleftharpoons MoO_2(OH)_2 \quad (4)$$

Both MoO_3 and $MoO_2(OH)_2$ should be very volatile compared with ZrO_2 and therefore allow a separation from it.
For the volatilization experiments an arrangement was applied as depicted in fig. 2. Air was saturated with water vapour at definite temperature and then led over the zirconium foil. In some experiments dry air was used instead of moist air.

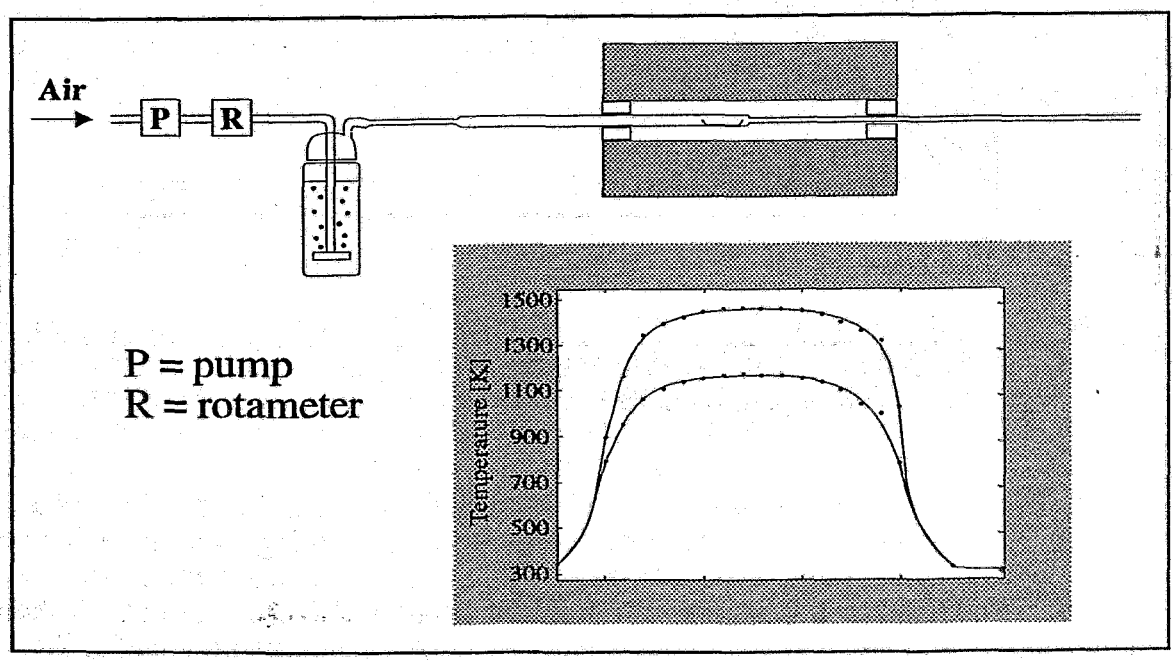

Fig. 2: Schematic of the set-up for the volatilization

About 0.2 g zirconium foil were heated up to 1170 K for 30 minutes in an air stream of 5 - 10 $l \cdot h^{-1}$ whereby the zirconium foil was oxidized. The molybdenum activity remaining in the zirconium dioxide was measured off-line by γ-spectrometry.
In a first series of experiments the temperature was increased step by step from 1170 K to 1470 K. Below 1470 K the release of molybdenum was ≤5 % within an hour. That's why subsequent investigations dealing with the dependence of the volatilization on humidity of air were carried out at the maximum of 1470 K. Results are shown in Fig. 3.

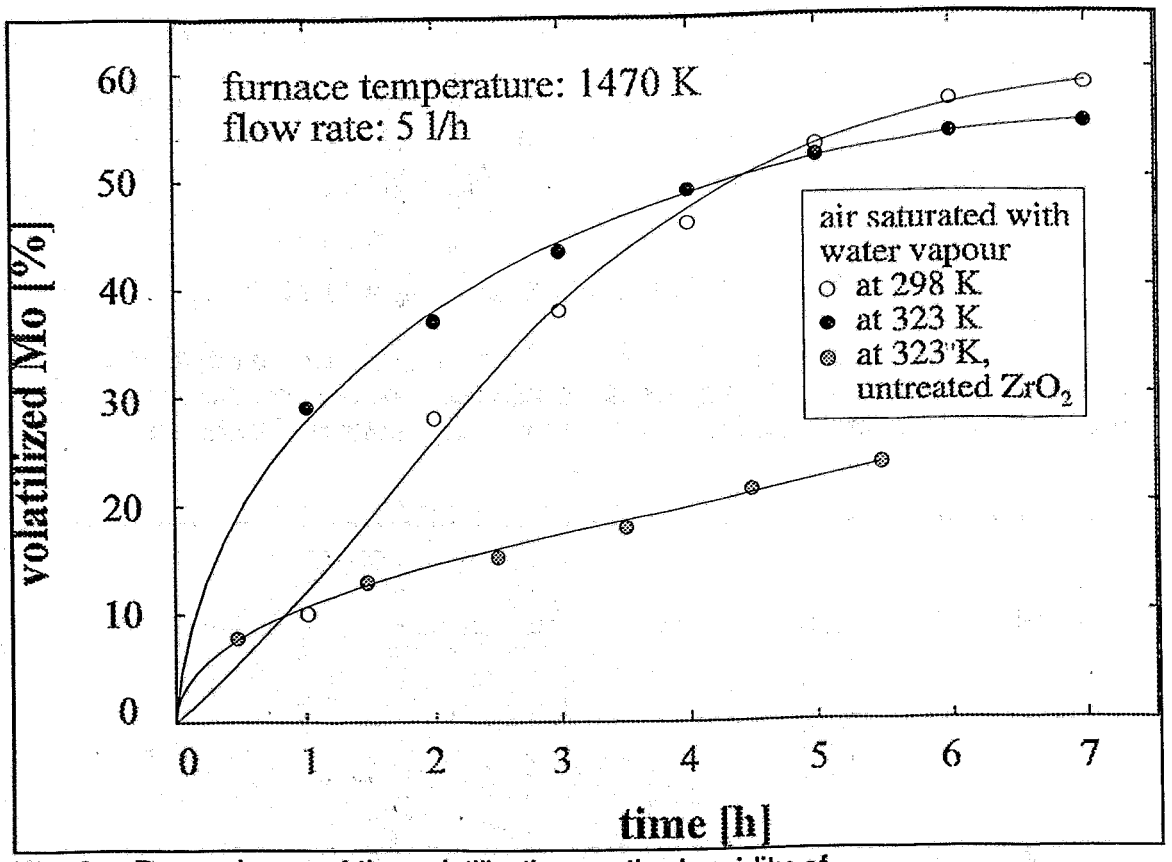

Fig. 3: Dependence of the volatilization on the humidity of air and the homogenization of ZrO_2

With dry air only 3 % of the molybdenum were volatilized within 2.5 h. With increasing humidity of air an increasing release was observed corresponding with the formation of $MoO_2(OH)_2$. For air saturated with water vapour at 323 K the evaporation from homogenized ZrO_2 was compared with that from untreated ZrO_2. The volatilization from treated ZrO_2 was much higher. Obviously due to the disturbance of the ZrO_2-structure volatile compounds are better delivered.
From these experiments one can conclude that the volatilization of carrier-"free" molybdenum from zirconium dioxide is possible. A high humidity of air and homogenized zirconium dioxide promote the evaporation.

Acknowledgement

These studies were supported by the Bundesminister für Forschung und Technologie of the Federal Republic of Germany under contract 06 DR 101 D.

VOLATILIZATION AND GAS PHASE TRANSPORT OF ELEMENT 106 IN HUMID OXYGEN

B. Eichler, H.W. Gäggeler,
Paul Scherrer Institute, CH-5232 Villigen PSI

S. Hübener
Research Center Rossendorf Inc., Institute of Radiochemistry

It is assumed that in an O_2/H_2O atmosphere element 106 forms a solid trioxide which is in equilibrium with the free acid in the gaseous state, as is well known for the chemical homologs Mo and W. In the case of single atoms the dissociation of the free acid can be considered as a dissociative adsorption process:

$$H_2\,106\,O_{4(g)} \rightleftharpoons 106\,O_{3(ads)} + H_2O \qquad (1)$$

The transportation rate of element 106 in a O_2/H_2O carrier gas depends on the position of equilibrium (1), which is determined by the partial pressure of H_2O as well as by the surface properties of the chromatographic tube, i.e. the thermodynamic adsorption and desorption functions. For the standard enthalpy ($\Delta H^\circ_{d.a.}$) and the standard entropy ($\Delta S^\circ_{d.a.}$) of the dissociative adsorption the following equations hold /3/:

$$\Delta H^\circ_{d.a.} = \Delta H^\circ_f[H_2O_{(g)}] + \Delta H^\circ_f[106\,O_{3(g)}] - \Delta H^\circ_f[H_2\,106\,O_{4(g)}] + \Delta H^\circ_{ads}[106\,O_3] \qquad (2)$$

$$\Delta S^\circ_{d.a.} = S^\circ[H_2O_{(g)}] + S^\circ[106\,O_{3(g)}] - S^\circ[H_2\,106\,O_{4(g)}] + S^\circ_{ads}[106\,O_3] \qquad (3)$$

Fast gas adsorption chromatography experiments have been proposed for the characterization of volatile compounds of element 106. The conventional descriptions of gas chromatographic separations are based on the assumption of constant chemical form during the chromatographic process /1,2/. In case of dissociative adsorption the dissociation process has to be taken into account. Equation (4) gives the theoretical description of a transport along a thermochromatographic column under such conditions:

$$t_r = \frac{a\,T_0\,c^0_{ads}\exp(\Delta S^0_{d.a.}/R)}{V_0\,g\,c_{H_2O(g)}}\left[Ei^*\left(\frac{-\Delta H^0_{d.a.}}{T_D}\right) - Ei^*\left(\frac{-\Delta H^0_{d.a.}}{T_s}\right)\right] \qquad (4)$$

and equation (5) for an isothermal column:

$$t_r = \frac{z\,d\,T_0}{V_0\,T}\left[1 + \frac{a_1\,c^0_{ads}}{V_1\,c_{H_2O(g)}}\exp\left(\frac{-\Delta H^0_{d.a.}}{RT}\right)\exp\left(\frac{\Delta S^0_{d.a.}}{R}\right)\right] \qquad (5)$$

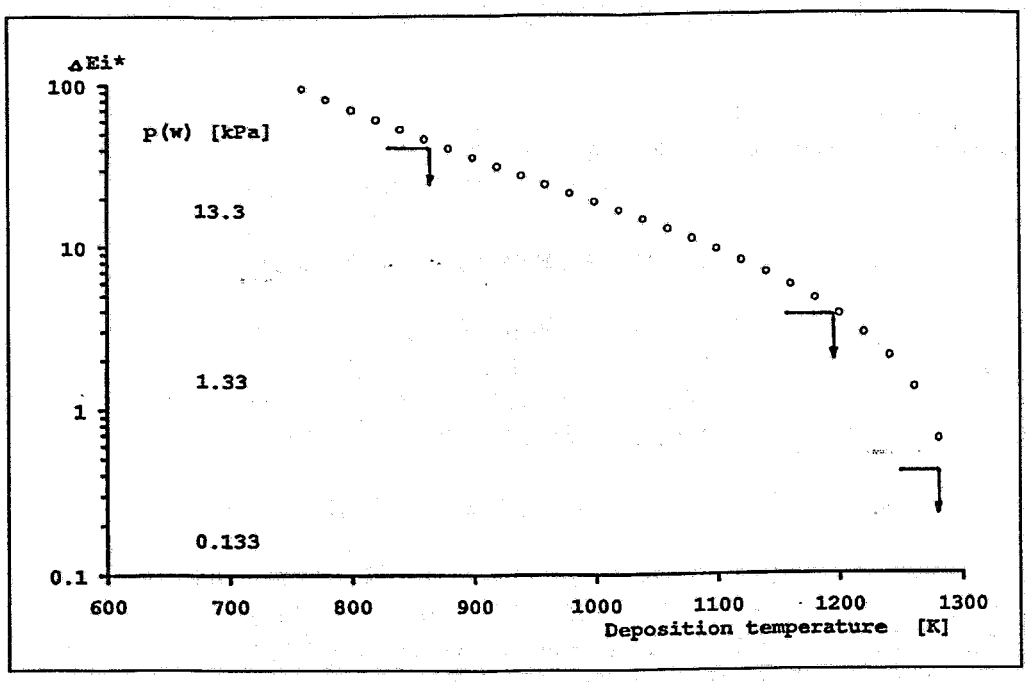

Fig. 1: Calculated deposition temperatures of element 106 in humid oxygen in a thermochromatographic column for three different H_2O partial pressures (arrows) and the experimental parameters given in Table 1.

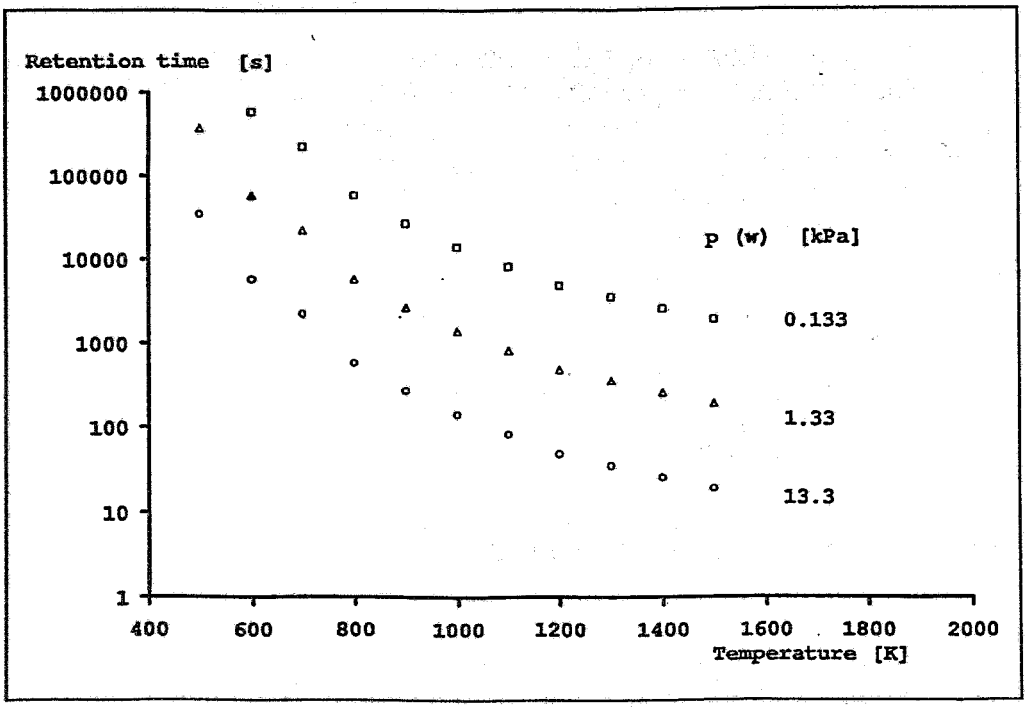

Fig. 2: Calculated retention times of element 106 in humid oxygen in an isothermal column as a function of the temperature and the partial pressure of the water vapour in the carrier gas.

Thermodynamic data for element 106 compounds are summarized in Table 1. They were obtained by extrapolations /5/ as well as by some assumptions about typical experimental conditions.The results of the calculations are depicted in Figs. 1 and 2. As is clearly evident, the oxygen carrier gas should be saturated with water vapour in order to obtain fast and efficient transport at (for quartz columns) maximum temperatures of about 1400K.
In a gas chemical experiment with O_2/H_2O as carrier gas element 106 should be well separable from the elements 104 and 105 as well as from heavy actinide elements since under such conditions these latter elements do not form volatile compounds.

Standard Data	
ΔH°_{ads} - Enthalpy of dissociative adsorption:	-40.0 kJ/mole /5/
ΔS°_{ads} - Entropy of dissociative adsorption:	-35.3 J/K mole /5/
$c^\circ_{ads}[H_2O_{(g)}]$ - Surface concentration:	$2.679*10^{14}cm^{-2}$
T_0 - Temperatur:	298K

Experimental parameters		
$c[H_2O_{(g)}]$ Water concentrations:	$3.54*10^{14}cm^{-3}$	[=0.13 kPa]
	$3.54*10^{17}cm^{-3}$	[=1.3 kPa]
	$3.54*10^{18}cm^{-3}$	[=13 kPa]
v_0 - Carrier gas flow rate:	33.33cm s^{-1}	

	isothermal	gradient
d - Column diameter	1 mm	4 mm
z - Column length	300 mm	-
g - Temperature gradient	-	5 Kcm^{-1}
T_s- Start temperatur	-	1300 K
T_D- Deposition temperatur	-	-
t- Retention time	-	60 s

Table 1: Model parameters for the calculation of the chromatographic behaviour of element 106 in a quartz column with humid oxygen as carrier gas

References

/1/ B. Eichler, I. Zvara, Radiochim. Acta 30, 233(1982)
/2/ H. Gäggeler et al., Radiochim. Acta 38, 103(1985)
/3/ B. Eichler et al., Radiochim. Acta, 56, 133(1992)
/4/ B. Eichler et al., Radiochim. Acta, in print (1993)
/5/ B. Eichler, S. Hübener, H. Gäggeler, in preparation (1993)

THERMOCHROMATOGRAPHY OF CALIFORNIUM, EINSTEINIUM, AND FERMIUM IN METALLIC COLUMNS

S.Hübener
Research Center Rossendorf Inc., Institute of Radiochemistry

B.Eichler, H.Gäggeler
Paul Scherrer Institute, Laboratory for Radiochemistry, Villigen, Switzerland

M.Schädel
Gesellschaft für Schwerionenforschung mbH, Darmstadt

Thermochromatography in metal columns is a promising technique for the fast separation of heavy actinoids. However, analytical applications were limited due to admixtures of calcium, added in weighable amounts to stabilize the trace amounts to be separated in the elementary state /1/. In an earlier attempt to study the heavy actinoids under calcium-free conditions vacuum-thermochromatography has been used /2/.

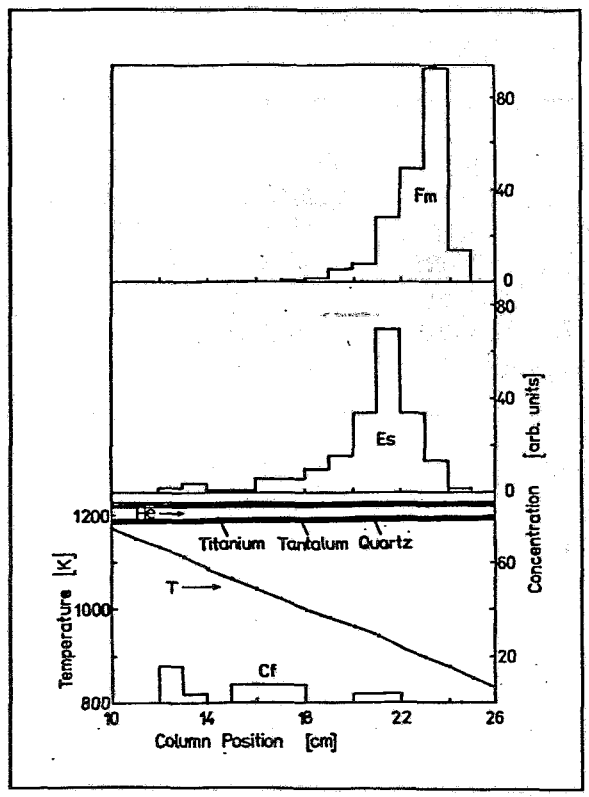

Fig. 1: Thermochromatographic distribution of Cf, Es, and Fm in a titanium column.

In the present work the heavy actinoid fraction of experi-ments which were carried out to investigate further the chemical properties of element 105 at the UNILAC of the GSI /3/ was used to study the thermochromatography of Cf, Es, and Fm in titanium, molybdenum, and tantalum columns under calcium free conditions using high-purity helium as a carrier gas.

The experimental procedure was very similar to that described earlier in detail /1/. The actinoids under study were evaporated from a molten lanthanum/aluminium alloy into a titanium pre-column. At 1275 K the evaporated actinoid atoms entered with the carrier gas the open tubular thermochromatographic column (inner dia-meter 3 mm). The column was held at working temperature for 30 minutes. The distribution of the actinoids along the thermochromatograhic column was measured off-line by alpha spectrometry in 1 cm sections. Among others ^{248}Cf, ^{249}Cf, ^{252}Es, ^{253}Es, and ^{255}Fm were used as the indicatory isotopes.

A schematic of the columns used and the thermochromatographic distribution in titanium and molybdenum columns are shown in Fig.1 and Fig.2, respectively.

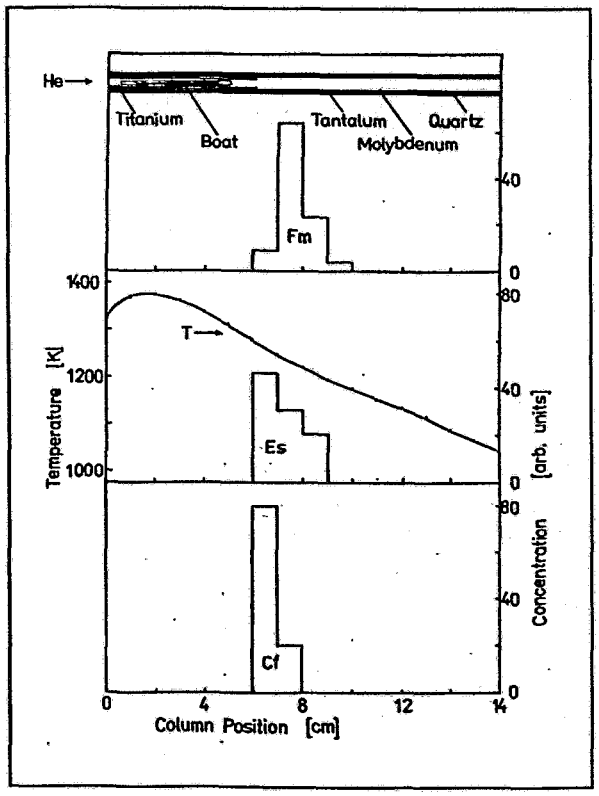

Fig. 2: Thermochromatographic distribution of Cf, Es, and Fm in a molybdenum column.

In molybdenum and tantalum columns the actinoids Cf and Es were deposited immediately after having left the pre-column, obviously at the first contact with the metallic surface. Fm was deposited at 1225 K in molyb-denum columns and at 1200 K on tantalum. In titanium columns Es and Fm were transported down to 930 K and 890 K, respectively, whereas Cf was lost due to diffusion into the titanium bulk.

Enthalpies of adsorption evaluated from the experimental data are summarized in Table 1. For the adsorption of Cf and Es on Mo and Ta only lower limits are given. Theoretical enthalpies of adsorption on titanium calculated on the basis of an empirical model are given for comparison /4/.

As follows from these data also under calcium free conditions titanium can be used as a container or tube material for the gaseous phase transport of Es and Fm at temperatures above 1000 K and as column material for their chromatographic separation. Thermochromatographic studies in columns made of Mo, Ta, or other transition metals should be continued at higher temperatures.

Table 1: Thermochromatographic deposition temperatures T_{ads} and enthalpies of adsorption $-\Delta H_{ads}$

Actinoid	Cf		Es		Fm	
Adsorbens metal	T_{ads} [K]	$-\Delta H_{ads}$ [kJ/mol]	T_{ads} [K]	$-\Delta H_{ads}$ [kJ/mol]	T_{ads} [K]	$-\Delta H_{ads}$ [kJ/mol]
Mo	≥1260	≥307.9	≥1250	≥301.3	1225	290.6
Ta	≥1260	≥302.1	≥1260	≥302.1	1200	277.3
Ti	Diffusion		930	219.2	890	210.2
$Ti_{(calc.)/4/}$		283.4		214.7		210.4

Acknowledgement

These studies were supported by the Bundesminister für Forschung und Technologie of the Federal Republic of Germany under contract 06 DR 101 D.

References

/1/ S.Hübener, I.Zvara
Radiochim. Acta 31, 89 (1982)
/2/ B.Eichler, G.V.Buklanov, S.N.Timokhin,
Kernenergie 30, 469 (1987)
/3/ A.Türler et al.
PSI Annual Report 1992, Annex III A, 95
/4/ B.Eichler, S.Hübener, H.Roßbach
Report ZfK-560 (1985)

3. ECOLOGICAL RESEARCH

MINING RELICS AS SOURCES OF NATURAL RADIOACTIVITY
II. RELEASE OF RADON FROM URANIUM MILL TAILINGS

L. Baraniak
Research Center Rossendorf Inc., Institute of Radiochemistry

A. Mende
Nuclear Engineering and Analytics Inc., Rossendorf

Large open storage areas of tailings from fourty years uranium mining and milling in Saxony and Thuringia endanger the envi-ronment by the release of natural radioactivity and other toxic substances. An essential part in risc assessment for the near field surroundings plays the radiation exposure of human respiratory tract (larynx and lung) by ^{222}Rn and its daughters /1/.

To provide data for the first estimation a series of radiological measurements concerning the Rn flux and activity of ^{226}Ra were carried out on the tailings basin No.4 in the "Hüttengrund" near Freital (Fig.1, Tab.1). The results have been used to adjust the coefficients of the interstitial diffusion equations. Therefore the specific Radon flux (J *per Bq* ^{226}*Ra/g*) was calculated in dependence on the tailings layer thickness (L) for different diffusion coefficients (D_{Rn}) (Fig.2) /2/ according to

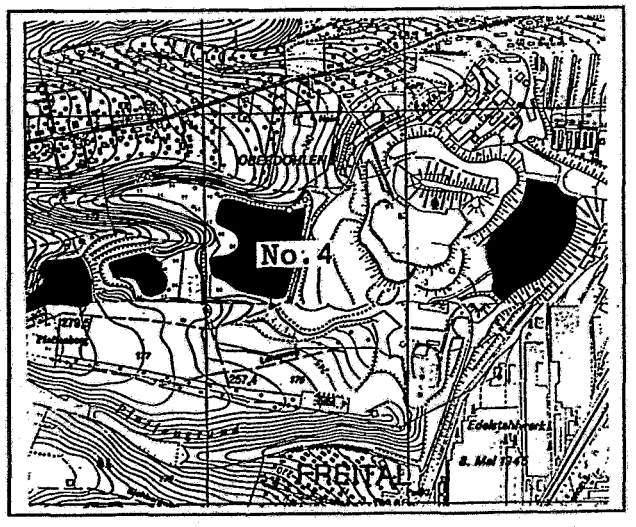

Fig. 1: Tailing storage ground at Freital near Dresden

$$\frac{\partial(\lambda_{Rn}c^{*}_{Rn})}{\partial t} - D_{Rn}\frac{\partial^2(\lambda_{Rn}c^{*}_{Rn})}{\partial x^2} + \lambda_{Rn}(\lambda_{Rn}c^{*}_{Rn}) - K_{Rn}\lambda_{Rn}(\lambda_{Ra}c_{Ra}) = 0 \quad (1)$$

Applying the boundary conditions $c_{Rn}=0$, $x=0$ and $(dc_{Rn}/dx)=0$, $x=L$ the solution for $0 \le x \le L$ and the flux $J_{Rn}=D_{Rn}(dc_{Rn}/dx)_{x=0}$ from material of the density ϱ can be written

$$J_{Rn} = \frac{K_{Rn}\lambda_{Rn}\varrho\, c_{Ra}}{\sqrt{\lambda_{Rn}/D_{Rn}}} \tanh L\sqrt{\lambda_{Rn}/D_{Rn}} \quad (2)$$

Table 1: Measured data and related diffusion coefficients

Specific activity	Exhalation rate		Diffusion coefficient
A, ^{226}Ra [Bq/g]	J$^{(*)}$, ^{222}Rn [Bq/cm^2*s] (*10^5)	per Bq(Ra)/g (*10^6)	D, eff. [cm^2/s] (*10^5)
10.3	3.889	3.776	1.038
13.5	5.833	4.321	1.317
11.2	5.139	4.588	1.510
15.3	6.111	3.994	1.169
9.7	4.167	4.296	1.317
7.3	3.333	4.566	1.510

The corresponding measured data have been put into the plot in order to find the real diffusion coefficients in this graphical way (bar in Fig.2).

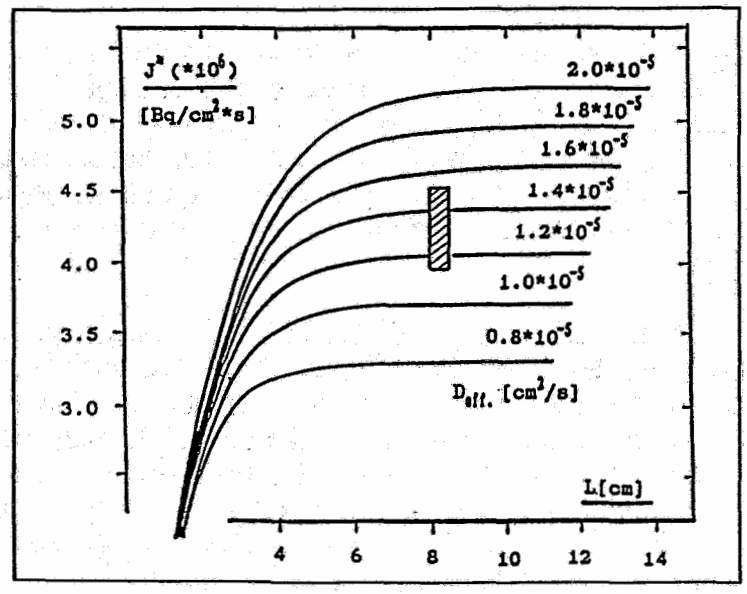

Fig. 2: Plot of J^* against L in dependence on D_{Rn}

It results an average $D_{eff.}$ of

(1.31±0.17)*10^{-5}cm^2/s,

three orders of magnitude less than for soils and the characteristic tailings layer penetration distance of about 10 cm.

Despite the high ^{226}Ra content the low Rn diffusibility in the tailings causes the exhalation rate to be only the 30 fold of normal soils.

References

/1/ U.S. Environmental Protection Agency, EPA-Pamphlet OPA 86004 (August 1986), "A Citizens Guide to Radon"

/2/ A. Busigin, J.S. Nathwani, C.R. Philips Health Phys. 36, 393 (1979)

ACID FORMATION BY AUTOXIDATION OF SULPHIDE ORES AND THE INFLUENCE ON THE SOLUBILITY OF ORE COMPONENTS

H.-J. Engelmann
Research Center Rossendorf Inc., Institute of Radiochemistry

The richness of the Saxon "Erzgebirge" in productive ore deposits has lead to intensive exploitation of these deposits from middle age to present time. Thus, the originally tightly closed deposits were opened for agents of environment and their influences. Moreover, the topical interest in only one ore component as well as simple mining and extraction technologies lead to giant rockpiles. The crushed stones, which have a large surface and often contain toxic heavy metals, radioactive elements and sulphides, are exposed to the increasing industrial and natural (water, oxygen, erosion) influences of the environment. Subsequently, noxious substances are mobilised by chemical, biological and mechanical processes and infiltrated into surface water. The mines and tunnels remained after the exploitation are often flooded. Even the oxygen-containing water possibly causes mobilisation of toxic substances and their infiltration into the subsurface water.

Since sulphide minerals are exposed to atmospheric oxygen and water or water vapor a weathering process takes place. For example, in the case of pyrite sulphide is oxidised to sulphate, with sulphuric acid and Fe(II) ions being generated. In acidic solution Fe(II) is oxidised to Fe(III), which oxidises other ore components, e.g. uraniumdioxid, to soluble compounds. In addition, autotrophic micro-organisms (e.g. thiobacillus ferrooxidans) are known to promote oxidation and leaching of ores and minerals /1/.

The pathway of the mobilised compounds through the mines, and waterways is determined by the actual environment. Since the chemical properties of the same element in different valency states vary widely, the migration behaviour of these elements depends strongly on the redox conditions. The oxidation state may be changed during the migration through the geosphere by reaction with dissolved and solid reactants. The redox capacity of the geosphere is present in the form of reducing minerals. This redox capacity can act by direct redox reactions of the solid with adsorbed ions or by dissolution of the solid and reaction in solution.

The thermodynamic properties of dissolved species and minerals can be used to compute solution-mineral equilibria. Many reactions in nature involve oxidation and reduction steps. Whereas the overall oxidation-reduction processes in the whole system are often too complex to treat quantitatively, a large number of half-cells are known, or can be determined quickly.

Fig. 1 shows a generic Eh-pH diagram for environmental waters of different origin /2/. The pH of most natural waters lies between pH = 4 and 9. Waters from many mine and coal tailings are extremly acidic, comparable with a variety of waters accompanying chemical wastes. The individual fields in the diagram correspond to oxidising, transitional, and reducing environments. These, identified by numbers, are: (1) acidic and oxidising mine waters; (2) rain; (3) river water; (4) normal ocean water;

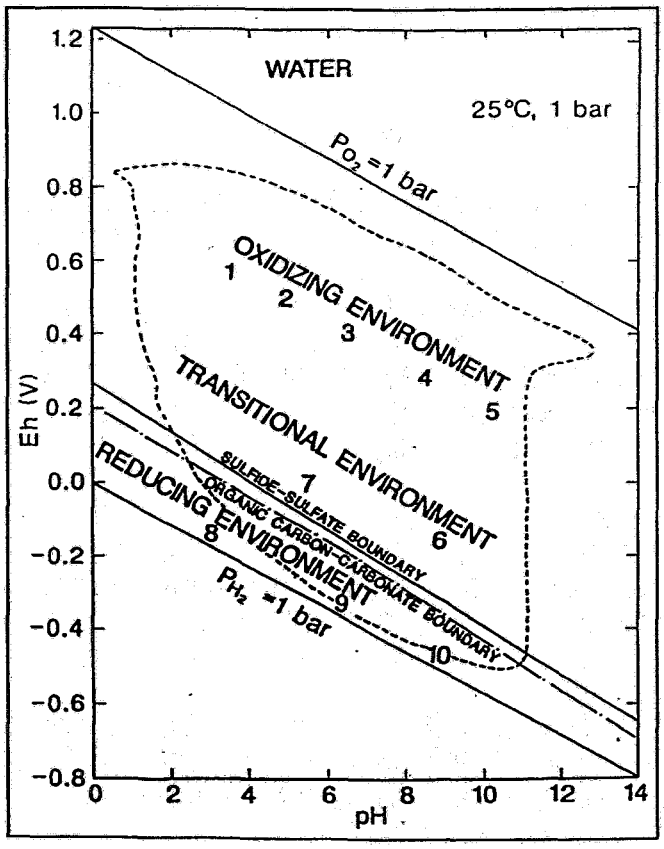

Fig.1: Eh-pH diagram of water /2/

(5) saline waters. There are two important boundaries in the diagram. The first is the line between reduced and oxidised sulphur species which separates metal sulphides from their sulphates. Mine waters are located above this line within the acidic range (e.g. uranium mine Schlema: pH = 4 - 6; sulphate = 2000 ppm). The second boundary separates the organic carbon from the carbonates. Eh-pH diagrams can not be used without reservation, because they assume equilibrium. In most cases very complex processes take place far from equilibrium and often no information is available on the kinetics.

The study of natural geochemical systems leads to a better understanding of the mobilisation, transport and retardation of radionuclides, heavy metals and toxic substances in the near as well as the far-field surroundings, and to the improvement of the thermodynamic data-bases and the transport codes such as CHEMVAL and PHREEQUE for the risc assessment of mining relicts and waste deposits /3/.

References

/1/ Trudinger, P.A.: Microbes, metals and minerals. Miner.Sci.Engng. 3, 13-25 (1971)

/2/ Brookins, D.G.: Eh-pH Diagrams for Geochemistry. Springer-Verlag, Berlin, (1988)

/3/ Chemistry and Migration Behaviour of Actinides and Fission Products in the Geosphere, Second Conference, Monterey, California, Nov. 1989 Radiochim. Acta 52/53, 413-518 (1991)

A SIMPLE BALANCE FOR WEATHERING OF ROCKS IN A ROCKPILE

G. Geipel
Research Center Rossendorf Inc., Institute of Radiochemistry

The investigated rockpile 250 in the town of Schlema, which had a volume of about $1*10^6$ m^3, had been leached for more then forty years by rain.

The content of radionuclides in the rockpile could be calculated by gamma-spectrometric measurements. If we assume that the volume of the dump is equal to $2*10^6$ tons of rocks and an average of 50 ppm U-238 (600 Bq/kg Th-234) is contained, then a sum of about 100 tons uranium-238 and 700 kg of U-235 are assessed. Other nuclides will be found in the order of kg, so 5 kg U-234 or 2 kg Th-230.

In Schlema it is raining about 800 mm every year. The rockpile had an area of 30.000 m^2. Corresponding to this, we calculated with $24*10^6$ l water. This rain water contains 8 mg/l sulphate (2000 moles per year), a pH of 4.3 (1200 moles of hydrogen ions) and 8 mg/l dissolved oxygen (6000 moles per year).

The fraction of cavities in the rockpile is assumed to be up to 35%. Neglecting diffusion of oxygen in from outsides, Up to $2.8*10^6$ moles oxygen there would be available for oxidising minerals over a time of 40 years (70.300 moles per year).
The most important reaction is the oxidation of pyrite /1,2/:

$$4\ FeS_2 + 15\ O_2 + 10\ H_2O \rightarrow 4\ FeOOH + 16\ H^+ + 8\ SO_4^{--} \qquad (1)$$

If we consider this reaction to be responsible for releasing sulphate ions, then 2.44 tons of this mineral will react in the rockpile every year bringing about 3.91 tons sulphate ions into solution.
The sulphate concentration of the trickle water was found to be 2 g/l. WISMUT Inc. measured at point 102 in Schlema values of about 3 g/l sulfate /3/. In the next step we calculate about $1.95*10^6$ l/a for the value of trickle water. This means that more than 90% of the rain will evaporate at the surface and in the upper parts of the rockpile.

The trickle water contains about 2 mg/l uranium. With the calculated trickle water of $1.95*10^6$ l/a 3.9 kg uranium will be leached per year. This means that 78 tons of minerals must be weathered, if the content was about 50 ppm uranium in the rocks.
The pH of the trickle water is 7-8, thus all input of hydrogen ions (rain and pyrite oxidation, 82.600 moles) must have reacted with minerals.
The stability of minerals against weathering is determined by its abrasion pH.

From gamma-spectrometric measurements we know that the trickle water contains about 0.23 g/l potassium ions.

One possible reaction is the weathering of Glimmer /1,2/:

$$\underset{\text{Muscovite}}{2KAl_2[AlSi_3O_{10}(OH)_2]} + 3H_2O + 2H^+ \rightarrow \underset{\text{Kaolinite}}{3Al_2Si_2O_5(OH)_4} + 2K^+ \quad (2)$$

For the balance 4.6 tons of potassium minerals must be weathered every year. The excess of 64.800 moles hydrogen ions will react with other minerals. From measurements at point 102 /3/ it is known, that trickle waters contain up to 0.51 g/l Mg^{++} and 0.35 g/l Ca^{++}.
For example, calcium and magnesium may be released by the weathering reaction:

$$\underset{\text{Tremolite}}{Ca_2Mg_5Si_8O_{22}(OH)_2} + 8H^+ \rightarrow 2Ca^{++} + 2Mg^{++} + 4SiO_2 + 4H_2O + \underset{\text{Talc}}{Mg_3Si_4O_{10}(OH)_2} \quad (3)$$

To achieve neutralisation the excess of hydrogen ions must react with 6.3 tons of this amphibolic mineral, leading to a solution with 0.33 g/l Ca and 0.2 g/l Mg.

The weathering of carbonate minerals is overlaid by precipitation of calcium carbonate. This explains the low carbonate concentration in the trickle waters.

With these ions we find a sum of 2.9 g/l salt. In nature the salt concentration is determined to be at 4-5 g/l. This shows that other weathering reactions have to be taken into consideration.

The sum of weathered minerals in this simple calculation reaches 13.3 tons, which is a smaller value then calculated from the uranium concentration in the trickle water.

To complete this simple balance it is necessary to know the values of evaporating and not draining rain and the concentrations of cations in the trickle water.

Acknowledgement

These studies were supported by the Bundesminister für Forschung und Technologie of the Federal Republic of Germany under contract KWA 1231 4.

References

/1/ P. Möller
Anorganische Geochemie, Springer Verl. Berlin, Heidelberg, New York, Tokyo, 1986, S.128 ff.
/2/ B. Mason; C. Moore
Grundzüge der Geochemie, Enke Verlag,Stuttgart, 1985, S. 143 ff.
/3/ Data from WISMUT, Chemnitz, 1991
/4/ R. Seim, G. Tirschendorf
Grundlagen der Geochemie, DVG, Leipzig, 1990, S.383

INVESTIGATIONS ON THE SOLUBILITY OF HEAVY METALS CONTAINED IN ROCKPILE MINERALS [1)]

G.Geipel
Research Center Rossendorf Inc., Institute of Radiochemistry

Rockpile materials contain a great number of heavy metals, which under natural conditions can be leached by rain. A first step for characterisation of the investigated materials is the determination of the mineralic contents of the rocks. Thin polishes of eleven samples, originating from the dump 250 in Schlema, were prepared[2)] and the stone-forming minerals were determined. The chief compo-nents in the stones are phyllite, quartzite, diabase, alaunic and siliceous slate. Several stone fractions show a high content of carbonate mine-rals. These minerals are important for the constant pH of the trickle waters.

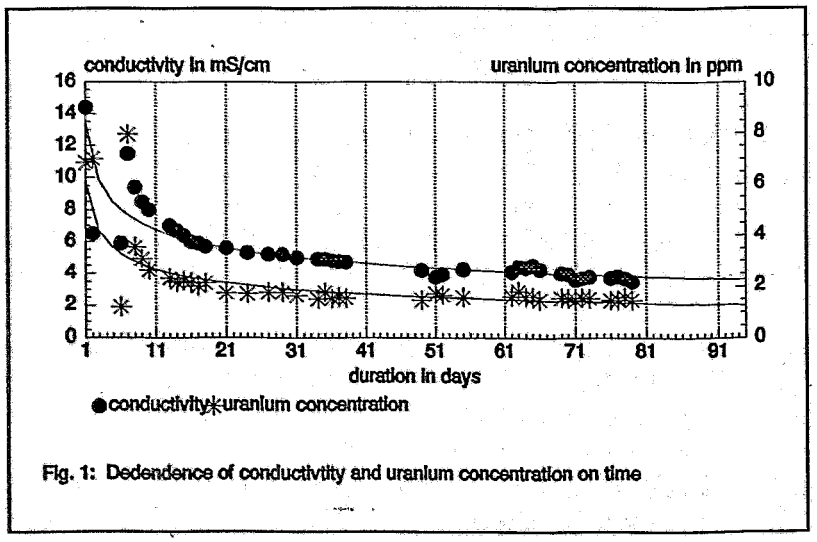

Fig. 1: Dedendence of conductivtity and uranium concentration on time

We have investigated the leaching rate of rocks. An amount of 20 kg of rocks was filled in a glass column of one metre length and 15 cm in diameter. Over a time of one year this column was eluated with normal deionised water. In this period we gave 130 portions of each 225 ml water to head of the column. Calculated for natural conditions this corresponds to 1670 mm rain per year, meaning twice the natural rate.

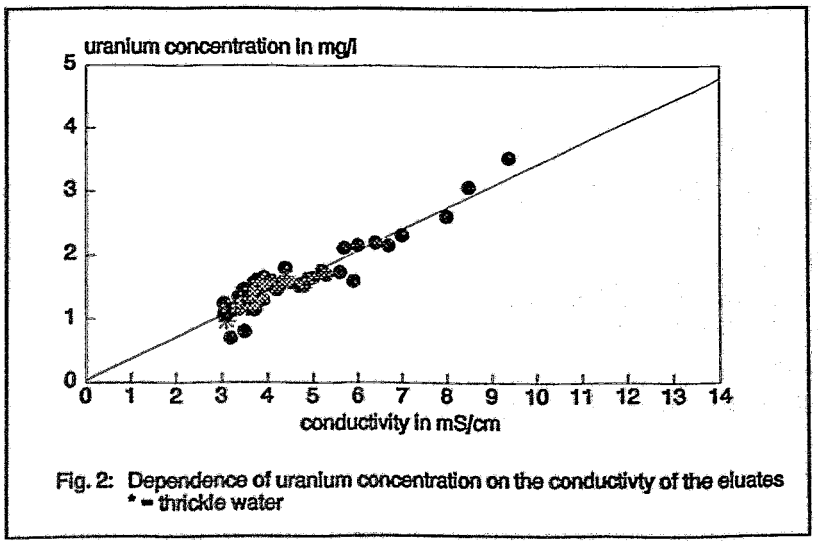

Fig. 2: Dependence of uranium concentration on the conductivty of the eluates
* = thrickle water

The solution leaving the bottom of the column was investigated for pH, dissolved oxygen, conductivity, concentrations of Pb (electrochemically) and U (spectrophotometrically) and for radionuclides (gamma-spectrometrically).
The pH and the concentration of the dissolved oxygen do not change with time. The pH of the solution

is buffered by the high content of carbonatic minerals in the column, so that the solution had everytime a pH of about eight. The constant dissolved oxygen could not decrease because we did not work in a glove-box.
Conductivity of the solution decreases with time, because of the decrease of dissolved salts in the column (Fig.1). In the short investigation time no weathering of rocks takes place, so that no production of soluble cations occurred.
By means of electrochemical methods we found no Pb in the solution. The simplest explanation for this phenomenon is, that no Pb is soluble, because all Pb ions were adsorbed on the surface of the rock material.
Uranium was determined using a spectrophotometric method /1/. During leaching the uranium content decreases in the same manner like the conductivity. Therefore we correlated the uranium content of the eluates with the conductivity of the solution (Fig.2).
The conductivity is not directly connected by the uranium content, because there are great amounts of other salts (alkali sulphate) which influence the conductivity. If we assume that the most important influence on the conductivity is caused by sodium and potassium sulphate and that these salts are connected by the weathering of rocks, then the result of this investigation means that the uranium content in trickle water mainly depends on the weathering of minerals.
The different behaviour of the heavy metal concentrations and conductivity reported earlier /2/, is caused by washout with sulphuric acid.

Acknowledgements

1) These studies were supported by the Bundesminister für Forschung und Technologie of the Federal Republic of Germany under contract KWA 1231 4.

2) Thin polishes and mineralogic determinations were carried out by Dr. W.Schmidt, Mining Academy Freiberg, Institute for Mineralogy.

References

/1/ D.A.Johnson, T.M.Florence
Anal. Chim. Acta 53, 73 (1971)
/2/ G.Geipel
Report FZR 92-08 (1992), p. 19

DISTRIBUTION OF SOME RADIONUCLIDES IN THE ROCKPILE 250 IN SCHLEMA

G. Geipel
Research Center Rossendorf Inc., Institute of Radiochemistry

In the last annual report we had shown the distribution of Uranium-238 (Th-234) in dependence of the depth and length of the rockpile. Continuing these determinations we determined the activity-concentrations of Th-230, if this was possible, of Ra-226, Bi-214 and Pb-210. If we compare all values for the ratio Th-230/Th-234(U-238) then an increase of this ratio with the depth is found (Fig.1) /1/. The conclusion is, that one or more nuclides between Th-234 and Th-230 must underlie a very high migration. Th ions are under conditions, existing in the dump (pH = 7), completely hydrolysed. These hydrolysed species do not migrate. They are coprecipitated with Fe hydrolysis products, for instance Goethit (FeOOH). Pa-234 has a too short half-life time to migrate over high distances.

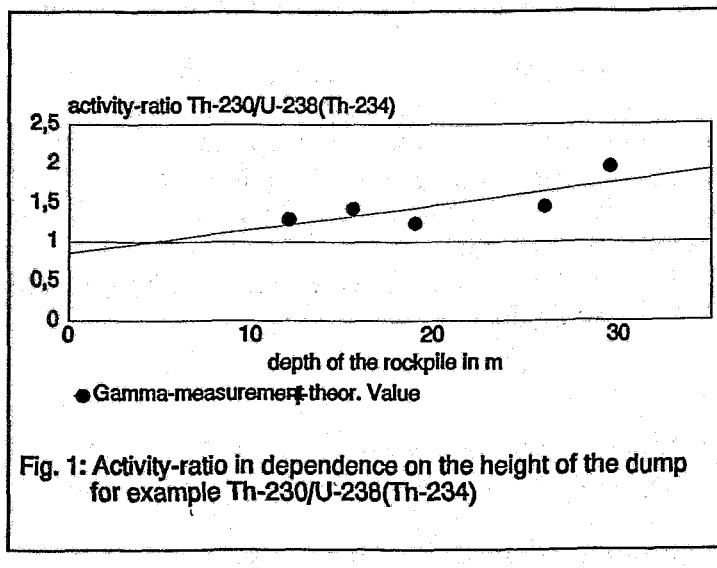

Fig. 1: Activity-ratio in dependence on the height of the dump for example Th-230/U-238(Th-234)

The only migrable ion is uranium-234. Starting from $^{238}UO_2$ the first alpha-decay leads to $^{234}ThO_2$, in which Th immediately is oxidised to the tetravalent state. The next two decays are beta-decays leading to pentavalent $^{234}PaO_2^+$ and hexavalent $^{234}UO_2^{++}$ /2/. This uranylion can migrate in the dump, if the uranium is on the surface of the rocks and there are no reducing conditions in the dump. In deeper parts of the dump the trickle water is undergone reducing conditions. Uranyl ions are reduced to tetravalent uranium, which hydrolyses and is sorbed to the rocks. The next decay leads to Th-230, with no migration properties.

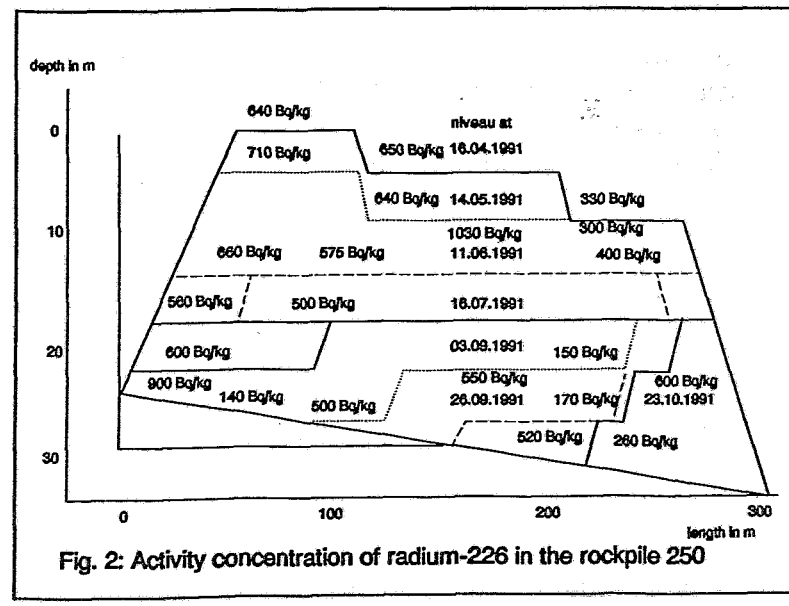

Fig. 2: Activity concentration of radium-226 in the rockpile 250

For Ra-226 we found

the same activity values like Th-230, therefore Th-230 and Ra-226 must be in equilibrium and no migration or the same migration took place for these both nuclides (Fig. 2). The activity of Pb-210 is in the same range like Ra-226. The only gaseous nuclide in this series is Rn-222. This nuclide can migrate in the other direction because of its transport to the atmosphere. Transport of radon in the inner of the dump will be small; most of the produced radon is in the inner of the rocks and the radon on the surface of rocks will be adsorbed. The nuclides between Rn-222 and Pb-210 have very short half-life times, so that no transport of these nuclides in the dump will take place.

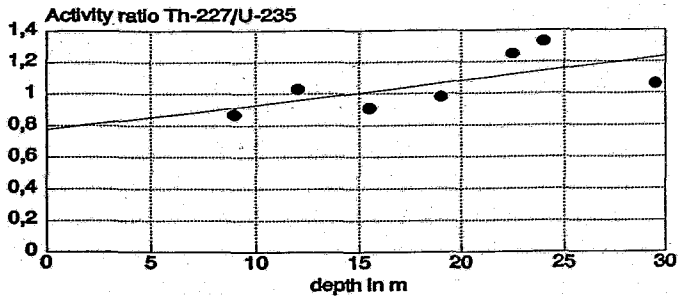

Fig. 3: Activity ratio of Th-227/U-235 in dependence on the depth of the rock

A second example for the increasing activity ratio in the rockpile is given in Fig. 3. The dependence of the ratio Th-227/U-235 on the depth is smaller then for Th-230/U-238, caused by the shorter half-life-times of Pa-231 and Ac-227 and their slower migration.

Acknowledgement

These studies were supported by the Bundesminister für Forschung und Technologie of the Federal Republic of Germany under contract KWA 1231 4.

References

/1/ M. Ivanovich
Radiochim. Acta 52/53, 257 (1991)

/2/ J.P. Adloff, K. Roessler
Radiochim. Acta 52/53, 269 (1991)

BATCH TESTING WITH INTEGRATED ANALYSIS - INTERACTION BETWEEN LEAD IONS AND GRANODIORITE

M. Thieme
Research Center Rossendorf Inc., Institute of Radiochemistry

In the field of the investigation of migration processes in rocks and soils a number of techniques are commonly used, such as batch, column, lysimeter, diffusion and high-pressure convection tests /1-5/. They are adapted in view of the issue to be solved. Hence, conclusions will be more or less specific. Batch tests often focus on determining distribution coefficients of any element-solid systems.
Together with other contributions in this report the paper presented here refers to investigations of the behaviour of harmful heavy-metal species contained in rockpiles of former uranium-mining activities. In order to gain a deeper insight into the kinetics of release and retention processes (de/adsorption, ion exchange, dissolution/precipitation, incor-poration /5/) batch tests have been performed using a specially designed apparatus. Its main component is a conical glass beaker provided with an inserted Rasotherm filter plate P 40 (pore width 16 - 40 µm). The arrangement allows both to supply a gas (air, N_2) for stirring and, if necessary, deaerating the mixture under investigation and to suckle a portion of the solution for its separate analysis. Thus, processing is considered to have distinct advantages in comparison to other batch-testing variants, e.g. shaking (abrasion of the solid) plus filtering (possible retention in the filter paper) or centrifugation (incomplete sedimentation under limited duration and speed). Further, the actual manner of separation generally consumes less time and allows an immediate continuation of the treatment. Moreover, an important feature consists in the integration of electroanalytical techniques in order to follow concentration changes: Connecting the beaker with a polarographic equipment (Metrohm 663 VA stand; AUTOLAB, Eco Chemie) heavy-metal concen-trations were *in situ* accessible as well as pH and specific con-ductivity could be continuously recorded using conventional sensors.

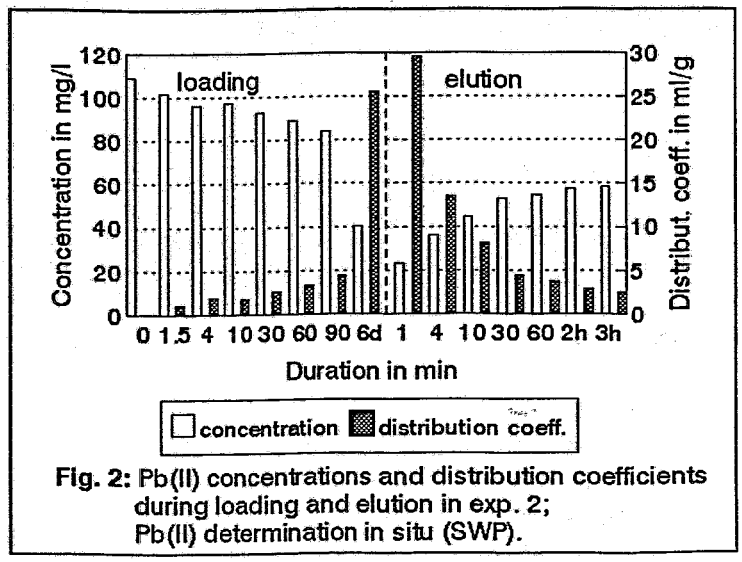

Fig. 2: Pb(II) concentrations and distribution coefficients during loading and elution in exp. 2; Pb(II) determination in situ (SWP).

First experiments aimed at testing the apparatus using granodiorite sand 0/2 mm and Pb(II) 1 - 100 mg/l in KNO_3 0.05 M, pH = 4.0 for loading, whilst KNO_3 0.05 M, acidified to pH = 2.0, was used as an eluent. Conditions and results of two experiments (1, 2) will be presented in the following.

Loading: starting value 100 mg l^{-1} (nominally), volume-to-mass ratio 15 ml g^{-1} (1: decreasing to 10.5 ml g^{-1} due to sampling), duration 4 h (1) and 141 h (2).
Rinsing: water, two portions, duration 5 min each.
Elution: number of portions two (1) and one (2).
Analysis: 1: pH - *in situ*, c_{Pb} - separately,
anodic stripping differential puls polarography (ASDPP);
2: c_{Pb} - *in situ*, square wave polarography (SWP).

In the course of loading, the interaction between solution components and the rock leads to an instant increase of pH and a consumption of dissolved Pb(II). The rates of these changes diminish with progressing duration, but continuate over several days at least. On the other hand, treating the loaded rock with a more acid solution (pH = 2) lead is released again. Summarising all partial amounts of lead $\sum(c_i\ V_i)$ dissolved in the solution fractions of loading, rinsing, elution and analysis (exp. 1) recoveries of 98.5% and 91.3%, respectively, were found. The lower value in the latter case will mostly be due to incomplete elution. Besides, a noticeable extraction of Pb(II) from the granodiorite may have been occurred in acid medium (ca. 2 mg l^{-1} in maximum).

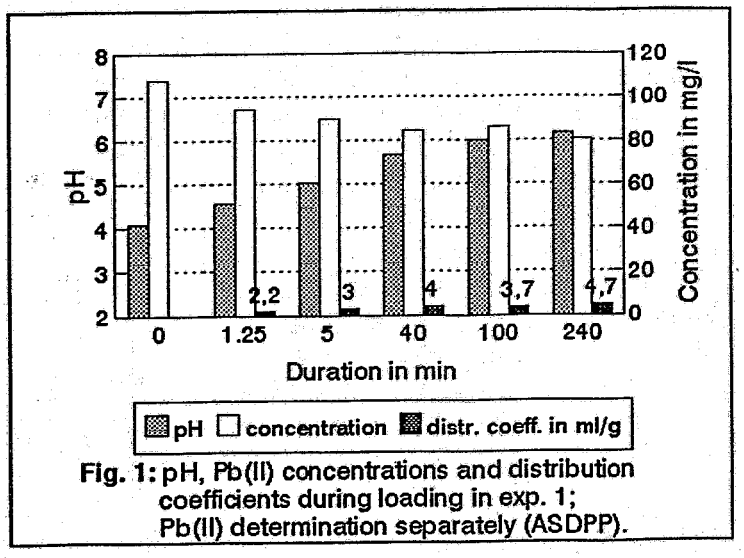

Fig. 1: pH, Pb(II) concentrations and distribution coefficients during loading in exp. 1; Pb(II) determination separately (ASDPP).

Distribution coefficients R_d of the ion i were calculated accor-ding to the formula $R_d=m_{ion,s}/(m_s{*}c_{ion,l})$ (index s denotes the solid phase, l - the liquid phase). The figures reflect the courses of R_d for both experi-ments. Taking into account that the homo-genity of the rock ma-terial is only limited the loading sections agree fairly well. Bode /5/ reported values of about 10^2 for long-time retention tests in systems of Pb(II) and triassic materials.

Acknowledgement

These studies were supported by the Bundesminister für Forschung und Technologie of the Federal Republic of Germany under contract KWA 1231 4.

References

/1/ B. Torstenfelt et al., Radiochim. Acta 44/45, 111 (1988)
/2/ J. A. Berry et al., ibid. 44/45, 135 (1988)
/3/ H. N. Erten, ibid. 44/45, 147 (1988)
/4/ D. Rancon, ibid. 44/45, 187 (1988)
/5/ W. Bode, GSF 16/89

CHEMOMETRIC ANALYSIS OF THE SPECTROPHOTOMETRIC DETERMINATION OF LEAD IN THE PRESENCE OF IRON(II)

M. Thieme
Research Center Rossendorf Inc., Institute of Radiochemistry

Investigations on the retention of toxic and radioactive species in rockpiles of former uranium-mining activities as well as the surrounding area require the application of suitable analytical methods. As for the determination of lead, there is a spectrophotometric method using 4-(2-pyridyl azo)resorcinol (PAR), which forms a red-coloured chelate complex in ammonia-NH_4Cl buffered medium /1/. However, its accuracy is affected in the presence of several metal ion species including Fe(II), which is rather abundant in rocks and soils.

Fig. 1 shows absorption spectra recorded under the conditions of the determination of lead with different Pb(II) and Fe(II) amounts. They reveal that Fe(II) gives rise to a peak located quite in the vicinity of that of Pb ($\Delta\lambda_p$= -18 nm). In order to quantify the actual influence of Fe(II) on the determination of Pb the amounts of both species (m_{Fe}, m_{Pb}) were varied as listed in the table below. The specified experimental results m^*_{Pb} are based on a calibration curve gained for iron-free conditions.

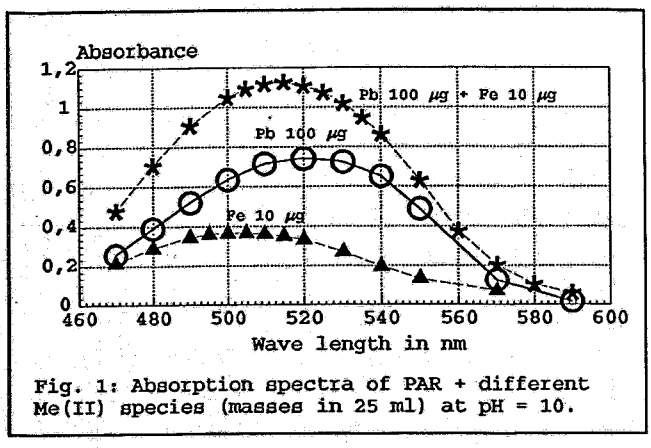

Fig. 1: Absorption spectra of PAR + different Me(II) species (masses in 25 ml) at pH = 10.

Table 1: Experimental results for the determination of Pb (m^*_{Pb}/µg; PAR, pH = 10, 25 ml, 530 nm) varying the amounts of Pb (as nitrate) and Fe(II) (as chloride).

m_{Pb}/µg	m_{Fe}/µg 0	10	30
0	0.5, 0.6	35.6, 40.8	108.5
5	5.3	43.2 #	111.2
12	11.8	49.1 #	112.9
50	50.0	86.0, 89.0	157.0
100	98.5	133.0,137.0	205.6

m_{Pb} lower than specified

The interfering influence of ferrous ions can be seen at a glance. A two-way analysis of variance (ANOVA), which was also performed according to the approach of Sarbu /1/, confirmed that both influencing factors are highly significant.

Thus, a linear model can be established, which quantitatively describes the respective effects and, moreover, allows to calculate the true amount of Pb, if that of Fe(II) is

known:

$$m^*_{Pb} = b_0 + b_1 m_{Fe} + b_2 m_{Pb} + b_3 m_{Fe} m_{Pb} + r_{Pb}$$

Using the matrix notation $\underline{Y} = \underline{\underline{X}}\underline{\underline{B}} + \underline{R}$, where
$\underline{\underline{X}}$ - design matrix, $\underline{\underline{B}}$ - matrix of coefficients,
$\underline{R}$ - matrix of residuals, $\underline{Y}$ - response matrix (results m^*_{Pb}),
the coefficients are calculated according to $\underline{\underline{B}} = (\underline{\underline{X}}^T\underline{\underline{X}})^{-1} * (\underline{\underline{X}}^T\underline{Y})$ (sum of squares of the residuals $SS_R = \underline{R}^T\underline{R}$ --> min):

$b_0 = 1.25$ µg, $b_1 = 3.58$, $b_2 = 0.981$, $b_3 = -0.00031$ µg^{-1}.

For examining the significance of b_3, SS_R was calculated both including all the coefficients and after neglecting b_3. The F test for the difference revealed that interactions between the factors were found to be not significant (b_3 --> 0!).
The results of the ANOVA are summarised in the following list:

Total sum of squares	$SS_t = 150\,046.8$ µg^2
SS corrected for the mean	$SS_{corr} = 35\,447.1$ µg^2
SS owing to the residuals	$SS_r = 43.3$ µg^2
SS owing to the model	$SS_{mod} = SS_{corr} - SS_r = 35\,403.8$ µg^2
SS owing to pure experimental errors	$SS_{pe} = 26.0$ µg^2
SS owing to the l.o.f.	$SS_{lof} = SS_r - SS_{pe} = 17.3$ µg^2
Correlation coefficient	$r^2 = SS_{mod} / SS_{corr} = 0.9988$
F test for l.o.f.	$F = [SS_{lof}/(15-3)]/[SS_{pe}/(19-15)] = 0.22$

The high value of the correlation coefficient indicates that only 0.12% of the variance is *not* described by the linear model, whereas the F value stated above reveals that the lack-of-fit is *not* significant in view of the contribution of the experimental errors to the residuals.
For a chemically meaningful description of the interference the atomic masses of both species should be taken into account. The ratio $b_1 M_{Fe} / b_2 M_{Pb}$ amounts to 0.985, i.e. the molar effect of Fe(II) on this special spectrophotometric determination of Pb is approximately as high as that of lead itself, which is, obviously, based on the same type of complexation.
It should be noted that the interference can be circumvented, e.g., by application of polarography also offering additional advantages.

Acknowledgements
The author thanks Mr E. Müller for programming the matrix operations and Mrs H. Neubert for performing the analyses. These studies were supported by the Bundesminister für Forschung und Technologie of the Federal Republic of Germany under contract KWA 1231 4.

References

/1/ O. G. Koch and G. A. Koch-Dedic,
Handbuch der Spurenanalyse, Berlin-Göttingen-Heidelberg-New York Springer 1964, p. 759.
/2/ C. Sarbu
Anal. chim. acta 271, 269-274 (1993).

A MODERNIZATION OF THE ZEISS M80 INFRARED SPECTROMETER

R. Nicolai
Research Center Rossendorf Inc., Institute of Bioinorganic and Radiopharmaceutical Chemistry

K.-H. Heise
Research Center Rossendorf Inc., Institute of Radiochemistry

We have linked the ZEISS Infrared-Spectrometer on type of M 80 (JENOPTIC CARL - ZEISS - JENA GmbH) with an efficient PC 486 DX/33 computer system and have found, that this combination is good suitable in a wide range of investigations in organic- and tracerchemistry.

The ZEISS IR-Spectrometer M 80 is a DIN-conformed double-beam instrument in the range of 4000 - 200 cm^{-1} with an average accuracy of 0,3 cm^{-1} and steering of optic grating. The computer coupling is realised by a V24 interface.

A specially adapted software version from ZEISS is designed for data management and data handling procedures. This software includes also an extensive library for spectras (SUSY) with a peak-search program and a "point to point"-comparsion. In tests we have investigated successfully many organic substances. The efficiency of the modernized device is demonstrated in figures 1 and 2 for any characteristic problems in laboratory practice.

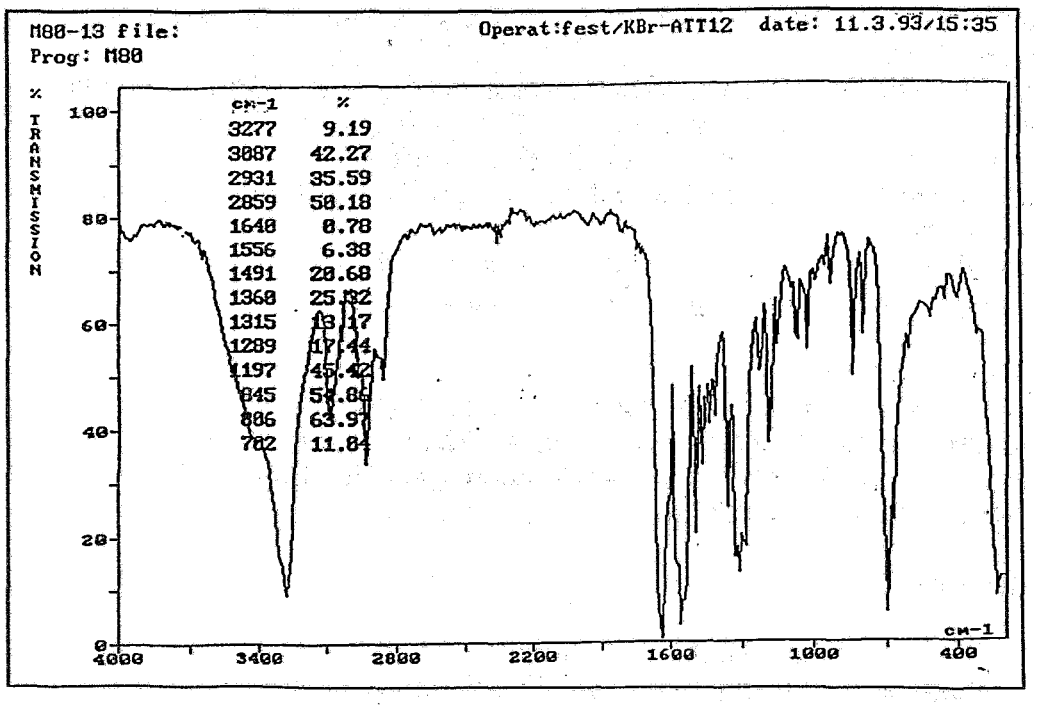

Fig. 1: Identification of an organic compound by means peak-search procedure

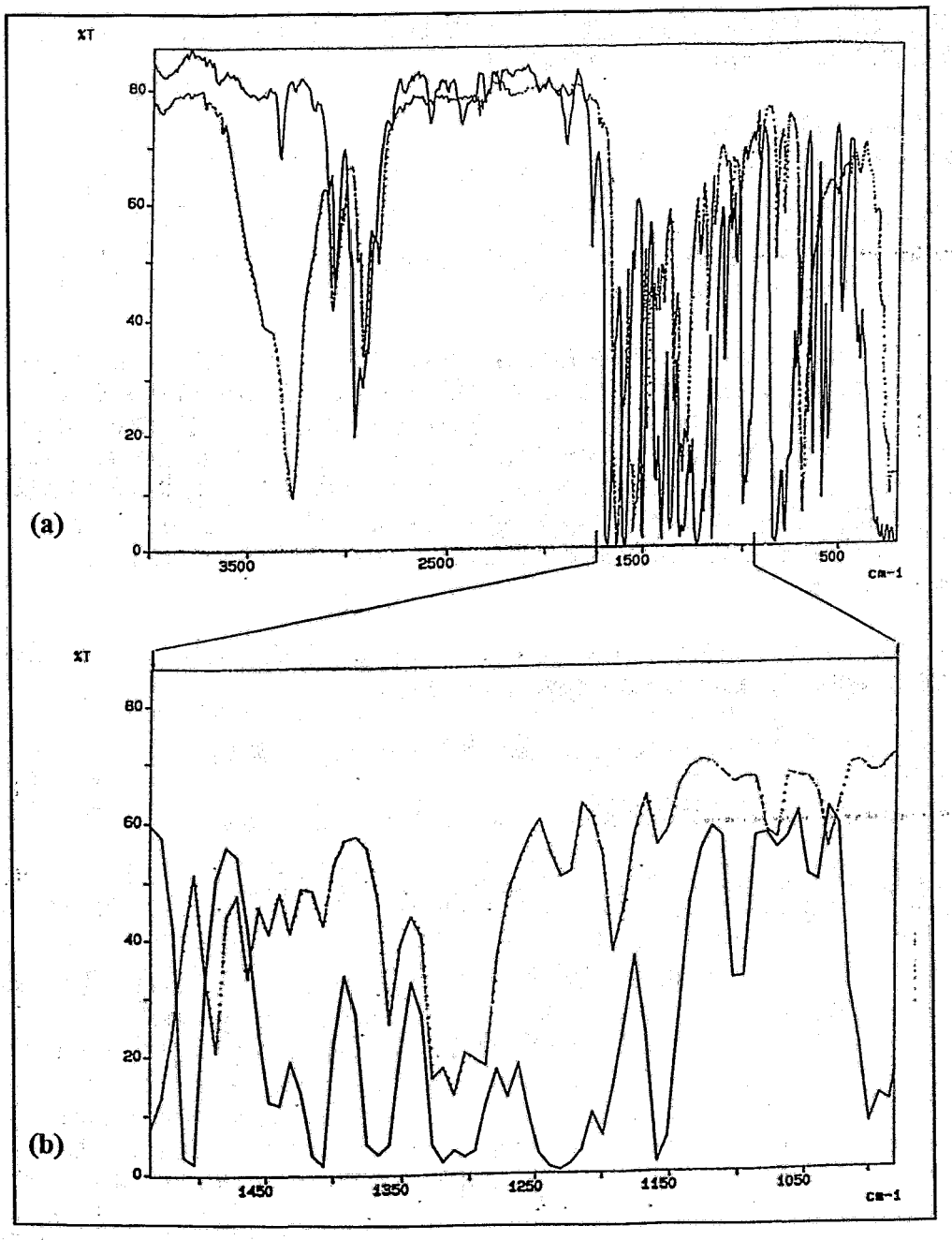

Fig. 2: Spectra-comparsion of two similar organic compounds for peak identification by overwriting procedure (a) and streching procedure in a select range (b) of high peak density

References

VEB Carl-Zeiss Jena: Rechnerkopplung M80/M85, 32-G342/24-1

Carl-Zeiss-Jena GmbH: Softwarehandbuch "Data Handling" M 82

Jenoptic Carl-Zeiss Jena GmbH: SPECORD M 82, 32-G344a-1

Jenoptic Carl-Zeiss Jena GmbH: Spektren-Such-System SUSY, 32-G344/21a-1

SINGLE-STEP-SYNTHESIS OF [1,2-^{14}C]TRICHLOROACETIC ACID STARTING FROM [1,2-^{14}C]POTASSIUM ACETATE

M. Bubner, K.-H. Heise
Research Center Rossendorf Inc., Institute of Radiochemistry

V. Vlasakova, K. Fuksova
Institute of Nuclear Biology and Radiochemistry
Czech Academy of Science, Prague

Modern trends in investigating tree damages have initiated an actual interest in [^{14}C]trichloroacetic acid with specific activities > 3,7 GBq/mmol /1,2,3/. Oxidation of representative volatile air pollutants, as the chlorocarbons 1,1,1-trichloroethane and tetrachloroethene, by UV-light leads to trichloroacetic acid. Their biotransformation can be examinated only by tracer technique. However, [1,2-^{14}C]trichloroacetic acid (I) of high specific activity is not commercially produced and the described methods for the synthesis of (I) are not feasible in a small scale synthesis (<1mmol) with a maximum of radioactivity.

Under the large number of radiosyntheses of (I) which have been described the following methods have been taken into account:

- the oxidation of [1,2-^{14}C]chloral with HNO_3 or H_2O_2 /4,5/
- the reaction of trichloromethyl-lithium with [^{14}C]CO_2 /10/
- the direct chlorination of acetic acid with sulfur and $FeCl_3$ or PCl_3 as catalysts /9/.

The first method is a multistep procedure starting from [1,2-^{14}C]acetate, [^{14}C]acetylene or [^{14}C]acetaldehyde /6,7/ and insuitable for small-scale synthesis.
The second method, a one step synthesis starting from [^{14}C]CO_2, leads only to a mono-[^{14}C]- substitution with a maximum activity of 2 GBq/mmol.
The third method has been proved only for technical processes and requires waterfree acetic acid. The last claim may be realized in the tracer technique only by addition of water binding substances as acetic anhydride with the consequence of a lower specific radioactivity.

Initiated by the publication of Abrams et al. /11/ and by our own experience in synthesis of [^{14}C]bromoacetic acid /12/ by direct bromination of [^{14}C]sodium acetate in presence of elemental sulfur, we developed a method for samall scale synthesis of (I).

[1,2-^{14}C]potassium- or sodium acetate of a maximum specific activity reacts in the presence of sulfur, red phosphorus and potassium iodide in a closed system (ampoule as a thick-wall reaction tube) quantitatively to (I). Isolation and purification have been arrived by sublimation or distillation of the solution in water or dioxane respectively. Radiochemical and chemical purity of the product was determined by RP-HPLC.

Experimental

1. Apparative equipment

The syntheses were performed using the standard vacuum-line and a special equipment /13/.
Reversed phase-HPLC analyses were performed using the multi-solvent delivery system WATERS 600 with programmable multiwave-length UV-detector and the BECKMAN 171 Radioisotope Detector.

2. Chemicals

[1,2-^{14}C]potassium acetate (from UVVVR, Prague) had a specific activity of 3,7 GBq/mmol.
Chlorine was self-made product from $KMnO_4$ and HCl. Other chemi-cals and solvents were p.a. quality delivered by MERCK and FLUKA.
The RP-18-phase columns on type of SGX C18 (7 µm) were made by TESSEK Ltd., Prague.

3. Synthesis procedure

A 30 ml-ampoule from thick-wall glass was charged with 0,1 mmol [1,2-^{14}C]potassium acetate in 1 ml methanol, 0,1mg phosphorus, 0,1 mg potassium iodide, and a solution of 2 mg sulfur in 2 ml benzene. The solvents were eliminated by lyophilisation leading to a very fine and homogenous mixture of all reaction components.

At the vacuum line 3 mmol waterfree (dried with P_2O_5) elemental chlorine was added und the ampoule was sealed by melting her up. The reactions were initiated by constant heating of the mixture at 180 to 190° C during 24 hours in a bath of boiling diethyleneglycol diethylether. Finally the volatile reaction products were condensed at the bottom of the ampoule by cooling down it with liquid nitrogen and heating the upper side with a burner. The ampoule was opened and immediately brought to the vacuum line. During the lyophilization at -80° C non reacted chlorine and hydrochloric acid were isolated from the reaction mixture. (I) is isolated from the ampoule by distillation.

Distillation of the pure undiluted substance includes high losses of yield. More successful is the distillation of solutions of (I) in water or dioxane. Like this from the starting activity may be isolated 70 - 80% in form of (I). The radiochemical purity of the product depends on the extent of chlorination and contains normally 2 to 10% of [1,2-^{14}C]dichloroacetic acid.

4. Analysis

For analysis is preferred the RP-HPLC using mentioned above equipment. The eluent was redistillited water, adjusted at pH 2.6 with sufuric acid and a flow-rate of 0,5 ml/min. UV-detection was made by 220 nm.

Results and discussion

[1,2-^{14}C]trichloroacetic acid is obtained according to the described method. Results of a serie of experiments, varying catalyst composition, the reaction temperature, and the reaction time are shown in table 1. The experiment no.10 represents the result of optimized conditions for a high-specific tracer synthesis.

Tab. 1 Synthesis of trichloroacetic acid from 0,1 mmol potassium acetate catalysed by 2 mg sulfur

No.	addit. catalyst	Cl_2 mmol	activity MBq	reaction temper. °C	time hours	analyt.result DCA[x] %	TCA[xx] %
1	without	1,0	0	>180	2 x 6	<50	<30
2	whitout	1,6	0	117	28	50	50
3	whitout	2,06	0	>180	2 x 7,5	>30	>50
4	without	2,06	0	>180	14	30	60
5	red P	2,0	<37	<180	3 x 6	50	30
6	KI/red	P 2,2	0	117	22	<5	<<5
7	KI/red	P 2,0	0	>180	4	50	50
8	KI/red	P 2,0	0	117/180	11/18	<5	>95
9	I_2/red	P 2,2	0	180	23		>98
10	KI/red	P 3,0	450	190	26	<10	>90

x) dichloroacetic acid
xx) trichloroacetic acid

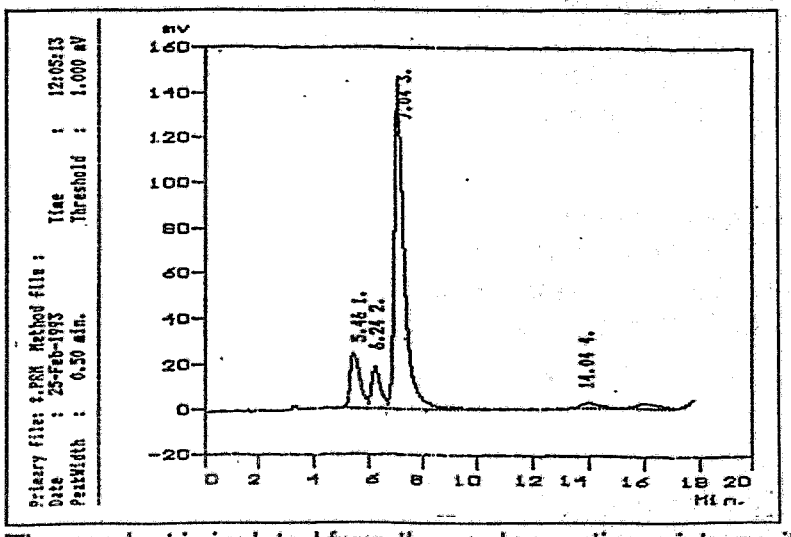

Fig. 1: Model HPLC-Chromatogram of trichloroacetic acid with impurities of mono- and dichloroacetic acid

The product is isolated from the crude reaction mixture with a yield of 80 to 90 %. The purification by distillation leads to

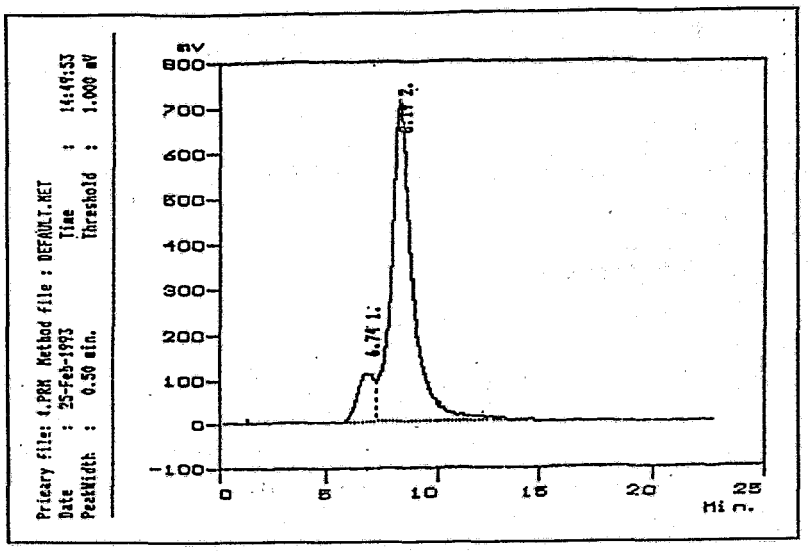

Fig. 2: HPLC-radiogram of the high-specific ^{14}C-labelled trichloroacetic acid

a further loss of material in range of 10%. Optimized reaction conditions lead to products of radiochemical purity of 90 to 98 %. Only labelled dichloroacetic acid is proved to be the radioactive byproduct. In figure 1 is shown a model HPLC-chromatogram of trichloroacetic acid with small impurities of mono- and dichloroacetic acid.
Figure 2 shows the HPLC-radiogram of the ^{14}C-labelled product.

For safety handling of the high specific labelled trichloroacetic acid were prepared 0,1 molar solutions in water or dioxane. Resolutions in alcohols can not be recommanded for the danger of esterification. Also dimethylsulfoxide as solvent is unsuitable as the acid spontaneously reacts to the dimethylsulfoxonium salt.

The neutralization of (I) should be done exclusively on temperatures < 0° C.

Trichloroacetic acid will be adsorbed very strong on glass-ware surfaces. Therefore for preparing dilutions of (I), e.g. for measuring of radioactivity, it is advisable to add some inactive substance.

References

/1/ Figge, K.,
Luftgetragene organische Stoffe in Blattorganen
Z. Umweltchem. Ökotox. 2, 200 (1990)

/2/ Frank, H., J. Vital, et al.
Oxidation of airborne C_2-chlorocarbons to trichloroacetic- and dichloroacetic acid
Fresenius Z. Anal. Chem. 333, 713 (1989)

/3/ Frank, H., A.Vincon, et al.
Montane Baumschäden durch das Herbizid "Trichloressigsäure" - Symptome und mögliche Ursachen
Z. Umweltchem. Ökotox. 2, 208 (1990)

/4/ Parkes, G.D., and R.G.W. Hollinghead,
The Preparation of Trichloroacetic Acid
Chem. Ind. (1954) 222

/5/ Boberg, H., K. Habenstein, et al.
Darstellung und katalytische Spaltung des Octachlor-(2-^{14}C)propan
Z. Naturforsch. 23b, 668 (1977)

/6/ Weaner, L.E., G.L.Burkhard, et al.
The preparation of chloral-1,2-^{14}C-hydrate
J. Labelled Compds. Radiopharm. 13, 141 (1977)

/7/ Pearce, G.W., and J.A. Jensen
Synthesis of DDT labelled with carbon-14 in the tertiary position
Science 118, 45 (1953)

/8/ Regula, S, J. Demiancok, et al.
CSP No.153,717

/9/ Sonia, J.A., and E.H. Scremin,
USP 2,674,620

/10/ Stock,M., A. Bernasch, et al.
Darstellung von [1-^{14}C]Trichloressigsäure
Isotopenpraxis 18, 260 (1982)

/11/ Abrams, D.N., R.C. Gaudreault, et al.
A Simple Synthesis of Radiolabelled Bromoacetic Acid
Appl. Radiat. Isot. 40, 251 (1989)

/12/ Jander, R. and M. Bubner
Synthese von ^{14}C-Bromessigsäure
Report FZR 92-08 (1992), p. 35

/13/ Bubner, M. and L.H. Schmidt,
Die Synthese Kohlenstoff-14-markierter organischer Verbindungen
VEB Georg Thieme, Leipzig, 1966

CHARACTERIZATION AND INVESTIGATION OF REACTIVITY OF HUMIC SUBSTANCES WITH RADIOTRACERTECHNIQUE - SUMMARY OF A STUDY

M. Bubner, K.-H. Heise
Research Center Rossendorf Inc., Institute of Radiochemistry

1. Introduction

During the last decades investigations on structure and influence of humic substances in soil and water environment became more and more important.
Chemical structures of humic acids and their content in organic matter of a given terrestrial ecosystem depends on the one hand on the specific ecological situation, on the other hand structure and concentration of humic acids decide the physical, chemical and biochemical processes in the soil and water environment.
Although accurate structures of humic acids due to their complexity and changeability are not attainable, reasonable estimates can be made on the composition and amounts of the various functional groups. SCHULTEN /2/, /3/, /4/ has presented on the basis of pyrolysis-soft ionization mass spectrometry model pictures of humic acid elements. Reviews about this topic are also given by McLAREN /6/, FLAIG /5/, ZIECHMANN /7/ and HAYES /1/.

Among the methods for determination of functional groups their derivatization in connection with NMR and IR analysis are practiced. The characteristic groups, introduced by derivatization with a specific reagent were determined and in this manner conclusions about the character and content of definite functional groups are possible. Comparing the character and amount of functional groups and the molecular weight of different humic acids it is possible to classify humic acid types.
Radiotracer in the field of humic acid investigations are useful in the following respects:

- in characterization of functional groups of definite humic acids
- in the tracertechnique with labelled humic acids.

2. The determination and characterization of functional groups

The derivatization of humic acids with radioreagents, as [^{14}C]-labelled diazomethane, methyliodide, acetic anhydride, trifluoromethyldiazoethane, trimethylsilylchloride, and meth- oxylamine in connection with radioactivity measurement has become practicable since equipments for quantitative oxidation of insoluble organic materials (as the oxidizers from ZINSSER or PACKARD) are commercially available. This method may be an alternative one for NMR and IR spectroscopic analysis.

3. Radiolabelling of humic acid for application in tracer technique

Humic substances - as humic and fulvic acids - have been shown to be important in the transport of organic and inorganic pollutants through the soil ecosystem. Radioisotope methods using radiolabelled pollutants as tracers have proved its worth in this field /8/, /9/, /10/, /11/, /12/, /13/.
However, such experiments do not provide information about the fate of humic acids in such very complex systems. Therefore a stabile labelling of humic substances, especially humic acids, would be necessary and should be a very useful completion of the known possibilities of investigation for use in environmental studies. Synthesis of labelled humic acids by covalent binding of the label ^{13}C or ^{14}C to a suitable part of the molecule is demanded.

The following possibilities to get labelled humic acids have been taken into consideration:

- [^{14}C]humic acids from natural material, resulting from increased ^{14}C-activity in the air due to the nuclear tests,

- [^{14}C]humic acids from humus fraction of decomposed ^{14}C-labelled plant material, made by growing of plants in a atmosphere of [^{14}C]CO_2 or by application of other labelled compounds, assimilated by plants /15/, /16/, /17/, /18, /19/,

- [^{14}C]humic acids prepared by co-polymerization of ^{14}C-labelled substrates on isolated humic acids /20/, /21/, /22/,

- [^{14}C]humic acid models by chemical syntheses /23/, /24/, /25/, /26/, /27/.

Substances, mentioned above proved to be suitable for degradation experiments and for studies in complexation and migration of humic acids. The maximum attainable specific activity is often very low and therefore limits their range of use.

Due to the chemical nature of this substances - their variety and local specificity - the obove mentioned humic acids and humic acid models may represent only its own behaviour in ecological systems. They are not representative for humic acids from other origin.

Solution of current problems in terrestrial environment demands labelling of definite humic acids of a given ecological system.

This may be realized only by a supplementary labelling of a given humic acid. The labelled humic acid must meet the following requirements:

- labelling must not singificantly change the physical and chemical properities (i.e. size, charge, metal complexing ability) of the original material,

- labelling must be irreversible in order to provide a stabile species,

- the biodegradability of the labelled group must be in the order of the original material, t.m. the groupe, containing the label must be whether preferential nor delayed microbially destroyed.

Often it is possible to came up to the first demand, if the chemical derivatization with a radioreagent of a maximum specific activity alter only a neglegible amount of the functional groups of the humic acid (e.g. -COOH, -OH, >C=O, >NR), whereby the reactivity and the size of the heavy molecule remains unchanged /19/. Such labelled humic acids may be used for complexation and migrations studies with metallics.

If the chemical and biochemical transformations of a humic acid bound xenobiotics should be studied, t. m. if also chemical changes of the humic acid skeleton must be taken into account, the labelling by derivatizating functional groups leads to misinterpretations of the experiments.

Derivable is therefore the labelling of humic acids at the molecule skeleton. This can be achieved by co-polymerization and covalent binding the label. Also known are enzymatically mediated incorporations of [^{14}C]aromatics /25/, /26/ as phenoles, amines, carboxylic acids etc.

CARLSEN /26/ describes also nonisotopic radiolabelling of humic acid with ^{125}J, ^{131}J and ^{36}Cl. Such labelled humic acid prove to be insufficient, due to the loss of label. Only carbon isotopes represent the skeleton of a humic acid, without any restriction.

It may be possible to label humic acids by ^{3}H with aid of the WILZBACH method very easy, bat C-H-bonds are not sufficiently stable for such tracer experiments.

Below the carbon isotopes ^{14}C is prefered to ^{13}C for its better detectability. Specific radioactivity of the radioreagent should be the high as possible in order to reduce the amount of changed structural elements in the humic acid skeleton and ensure a sufficient high activity for realization of tracer experimets.

References

/1/ Hayes, M.H.B., P. Mac Carthy, et al.
Humic Substances II, in "Search of Structure"
John Wiley & Sons, 1989, Chichester

/2/ Schulten, H.R., B. Plage, et al.
Chemical Structure for Humic Substances
Naturwiss. 78, 311 (1991)

/3/ Schulten, H.R. and M. Schnitzer
A contribution to solving the puzzle of the chemical structure of humic substances: pyrolysis soft ionization mass spectrometry
Sci. Total Environm. 117/118, 27 (1992)

/4/ Schulten, H.R. and M. Schnitzer
A State of the Art Structural Concept for Humic Substances
Naturwissenschaften 80, 29 (1993)

/5/ Flaig, W., H.Beutelspacher, et.al.
Chemical Composition and Physical Properities of Humic Substances in Soil Components; Vol.1, Organic Components, Springer, Berlin-Heidelberg-New York, 1975

/6/ Mc Laren, A.D. and G.H. Peterson (ed.)
Soil Biochemistry
Marcel Dekka, Inc., New York, 1967

/7/ Ziechmann, W.
Huminstoffe
Verlag Chemie, Weinheim/Bergstr., 1980

/8/ Szalay, A.
Cation Exchange Properities of Humic Acids and their Importance in the Geochemical Enrichment of UO^{2+} and other cations
Geochim. Cosmochim. Acta 28, 1605 (1964)

/9/ Kearney, P.C., D. D. Kaufmann. et al.
Biochemistry of Herbicide Decomposition in Soils
Soil Biochemistry 1, 318 (1967),

/10/ Bollag, J.M.
Microbial Transformation of Pesticides
Adv. Appl. Microbiol. 18, 75 (1974)

/11/ Azam, F., F. Führ, et al.
Fate of [Carbonyl-^{14}C]Methabenzthiazuron in an Arid Region Soil Effect of Organic Amendment, Soil Disturbance and Fumigation
Plant Soil 107, 149 (1988)

/12/ Murthy, N.B.K. and K. Raghu
Metabolism of ^{14}C-Carbaryl- and ^{14}C-1-Naphthol in Moist and Flooded Soils
J. Environ Sci. Health B24, 479 (1989)

/13/ Haider, K.M. and J.P. Martin
Mineralization of Carbon-14 Labelled Humic acids and of Humic Acid Bound Carbon-14 Xenobiotics by Phanerochaete Chrysosporium
Soil Biol. Biochem. 20, 425 (1988)

/14/ Scharpenseel, H.W., M. Wurzer, et al.
Biotisch und abiotisch gesteuerter Abbau von organischer Substanz im Boden
Z. Pflanzenern. Bodenk. 147, 502 (1984)

/15/ Brown, S.A. and A.C.Neish
Studies of Lignin-Biosynthesis using Isotopic Carbon
Canad. J. Biochem. 33, 948 (1956)
ibid. 34, 769 (1956)

/16/ Shields, J.A. and E.A. Paul
Decomposition of Carbon-14-labelled plant materials under Field Conditions
Can. J. Soil Sci. 53, 297 (1973)

/17/ Chesire, M.V., C.M. Mundie, et al.
Origin of Soil Polysaccharide Transformation of Sugars during the Decomposition in Soil of Plant Material Labelled with Carbon-14
J. Soil Sci. 24, 54 (1973)

/18/ Mandal, A.K. and M.B. Sen-Gupta
Transformation of Carbon-14-labelled Wheat and Berseem Plant Material in Different Indian Soils under Green-House Condition
J. Nucl. Agric. Biol. 10, 84 (1981)

/19/ Fustec-Mathon, E., P.Jambu, et al.
Analyse et Rote des Bitumes dans les Soils Sableux Acides
Soil Org. Matter Stud., Proc. Symp. Vienna 1977, 91

/20/ Dec, J. and J.M. Bollag
Microbial Release and Degradation of Catechol and Chlorophenols Bond to Synthetic Humic Acid
Soil Sci. Soc. Am. J. 52, 1366 (1988)

/21/ Dec, J., K.L. Shuttleworth, et al.
Microbial Release of 2,4-Dichlorophenol Bound to Humic Acid or Incorporated during Humification
J. Environm. Qual. 19, 546 (1990)

/22/ Arjmand, M. and H. Sandermann
Plant Biochemistry of Xenobiotics, Mineralization of Chloroaniline/Lignin Metabolites from Wheat by the White-Red Fungus Phanerochaete Chrysosporium
Z. Naturforsch. 41c, 206 (1986)

/23/ Adhikari, M.; P. Sen, et al.
Studies on Synthesis of Humic Substances in Laboratory under Different Conditions
Proc. Indian Natn. Sci. Acad. 51A, 876 (1985)

/24/ Bertin, G., M. Schiavon, et al.
Plant Bioavailability of Natural and Model Humic Acid Bound [^{14}C]Atrazine Residues
Toxicol. Environ. Chem. 26, 203 (1990)
/25/ Martin, J.P. and K. Haider
A Comparsion of the Use of Phenolase and Peroxidase for the Synthesis of Model Humic Acid-Type Polymers
Soil Sci. Soc. Am. J. 44, 983 (1980)
/26/ Carlsen, L., P. Lassen, et al.
Radiolabelling of Humic and Fulvic Materials for Use in Environmental Studies
Radiochimica Acta 58/59, 371 (1992)
/27/ Andreux, F., D. Golebiowska, et al.
D' un Modele Humique issue de L'autoxidation du Systeme Catechol-Glycine
Soil Org. Matter Stud., Proc. Symp.,Vienna 1976, 43

III. PUBLICATIONS, LECTURES AND POSTERS

PUBLICATIONS

G. Bernhard, H. Friedrich, W. Boeßert, A. Eckert
Untersuchungen zur Stillegung der Kernanlage AMOR-I des ZfK Rossendorf
Abschlußbericht zum Fördervorhaben BMFT - 02 S 73730 8
des Projektträgers Entsorgung 12/92

G. Bernhard, H. Friedrich, W. Boeßert, A. Eckert
Betriebsergebnisse und Untersuchungen zur Stillegung der Anlage zur
Molybdän-99-Produktion Rossendorf - AMOR-I -
Report FZR 93 - 04 (1993)

M. Thieme, D. Scharnweber, L. Drechsler, C. Heiser, B. Adolphi, A. Weiss
Surface Analytical Characterization of Chromium-Stabilized Protecting Oxide Layers
on Stainless Steel Referring to Activity Buildup,
J. Nucl. Mater. 189, 303 (1992)

M. Thieme, T. Stephan
Transformations of Titanium Carbide Precipitations under Hydrothermal Conditions,
Institute for Ion Beam Physics and Materials Research,
Report FZR 92-06, (1992), p. 51.

LECTURES

D. Rettig
The Experimental Programme of the SPAREX Loop
CEC Joint Research Centre Ispra, Institute for Safety Technology
Ispra, Italy, 30.01.1992

D. Rettig
The Experimental Programme of the SPAREX Loop
UKAEA Technology Winfrith, Chemical Physics Dept.
Winfrith, UK, 03.02.1992

G. Bernhard
Specific Interests of the Institute of Radiochemistry in the
Project "Biosorption of Uranium"
Rossendorf Meeting and Workshop about Biosorption
Rossendorf, 26.02.1992

G. Bernhard
Umweltforschung - eine Herausforderung für die Radiochemie
Festkolloquium " Zukunftsperspektiven von Rossendorf "
Rossendorf, 22.04.1992

G. Bernhard
Radiochemie im Spannungsfeld von Erzeugung, Anwendung und Entsorgung von Radioaktivität
Zentrumskolloqium "Forschungen in der Radiochemie"
Rossendorf, 27.06.1992

C. Nebelung
The solid electrolyte technique as a precise method for the investigation of reduction-oxidation-reaction
12th International Symposium on Microchemical Techniques
Cordoba Spain, 06.-11.09.1992

S. Hübener et al.
Gaschromatographic Studies with Short Lived Isotopes of Molybdenum and Tungsten
Third International Conference on Nuclear and Radiochemistry,
Vienna, 07.-11.09.1992

B. Eichler, S. Hübener
Chemical Transport Reactions of the Element 106 in the O_2-H_2O(g) and O_2-$(NO_3)_3$(g) - System
Third International Conference on Nuclear and Radiochemistry,
Vienna, 07.-11.09.1992

D. Rettig
In-situ-Verfolgung des Sauerstoffpotentials an reagierenden Metall/Gas-Grenzflächen
Discussion Meeting, Deutsche Bunsengesellschaft: "In-situ-In-vestigations of Physical Processes at Interfaces"
Lahnstein, 30.09.1992

H. Zänker
The Experimental SPAREX Loop
UKAEA Technology Winfrith, Chemical Physics Dept.
Winfrith, UK, 19.10.1992

H. Zänker
The Experimental SPAREX Loop
Centre d' Etudes Nucleaires de Caderache
Caderache, France, 29.10.1992

L. Baraniak and G. Geipel
Konzept der Grundlagenarbeiten zum Quell- und Ausbreitungsverhalten natürlicher Radioisotope in der sächsisch-thüringischen Bergbauregion
Seminarvortrag im Institut für Radiochemie,
Rossendorf, 12.11.1992

G. Bernhard
Untersuchungen zur Stillegung der Kernanlage AMOR-I des ZfK Rossendorf
II. Stillegungskolloquium des Institutes für Werkstoffkunde der Universität Hannover
Hannover, 19.-20.11.1992

H. Zänker
Fission Product Behaviour in the Primary Circuit of Severely Demaged Pressurized Water Reactors
Czechoslovak-German Workshop on Safety Research for VVER Reactors
Rossendorf, 24.11.1992

S. Hübener
Thermochromatographische Experimente am SAPHIR Gas-Jet
Seminar des Labors für Radiochemie, Paul Scherrer Institut,
Villigen, Würenlingen, 04.12.1992

G. Bernhard, D. Rettig, H. Zänker
Experimentelle Untersuchungen zum Spaltproduktverhalten im Primärsystem bei LWR-Kernschmelzunfällen
Workshop Spaltproduktverhalten, Köln, 08.12.1992

G. Bernhard
Profile in the Institute for Radiochemistry
Workshop Radiotracers in Biosystems, Rossendorf, 10.-11.12.1992

L. Baraniak, G. Geipel
Complexes and behaviour of radioactive and toxic heavy metals in the environment
Workshop Radiotracers in Biosystems, Rossendorf, 10.-11.12.1992

H. Zänker
Fission Product Behaviour in the Primary Circuit of Severely Demaged Pressurized Water Reactors
Workshop Radiotracers in Biosystems, Rossendorf, 10.-11.12.1992

POSTERS

M. Thieme, D. Scharnweber, L. Drechsler, C. Heiser,
B. Adolphi, A. Weiß
Oberflächenanalytische Charakterisierung von Schutzschichten auf rostfreiem Stahl, erzeugt durch hydrothermale Chromatbehandlung,
7. Arbeitstagung "Angewandte Oberflächenanalytik",
Jülich, 22.-25.06.1992; Kurzfass. S. 61.

G. Geipel
Untersuchungen zu toxischen und radiotoxischen Inhaltsstoffen der Halde 250 des ehemaligen Uranerzbergbaus in Niederschlema
Jahrestagung der Fachgruppe Umweltchemie und Ökotoxikologie der GDCh
Potsdam, 16.-17.11.1992

WORKSHOPS (organized by IRC)

Biosorption of Uranium
Rossendorf, 26.-27.02.1992

Spaltproduktransport im Primärkreislauf von LWR
Rossendorf, 21.07.1992

Spaltproduktverhalten in Reaktoren
Köln, 08.12.1992

Radiotracers in Biosystems
Rossendorf, 10.-11.12.1992

IV. TALKS OF VISITORS

Talks of visitors

F. Arendt
KfK Karlsruhe, Germany
Statement of KfK Karlsruhe
Workshop Biosorption of Uranium, 26./27.02.1992

L.R. Dole
ODGEN, USA
Identify issues to discuss
Workshop Biosorption of Uranium, 26./27.02.1992

B.D. Fisaon
DOE / ORNL, USA
US R&D experiences
Workshop Biosorption of Uranium, 26./27.02.1992

C.S. Higgins
ODGEN, USA,
Background of proposal development in biosorption study
Workshop Biosorption of Uranium, 26./27.02.1992

C.S. Higgins
ODGEN, USA
Requested German participation in Biosorption of Uranium
Workshop Biosorption of Uranium, 26./27.02.1992

T. Mayfield
DOE / ORNL, USA
General Description of the organization DOE / ORNL
Workshop Biosorption of Uranium, 26./27.02.1992

U. Morys
STEAG AG, Essen, Germany
General description of the organization Steag
Workshop Biosorption of Uranium, 26./27.02.1992

Sänger
Wismut AG, Engineering and Consulting, Chemnitz, Germany
Previous biosorption studies
Workshop Biosorption of Uranium, 26./27.02.1992

W.J. Schmidt-Küster
Energie Consult GmbH, Bonn, Germany
General description of the organization ODGEN IAEL
Workshop Biosorption of Uranium, 26./27.02.1992

K. Verfondern
Institut für Sicherheitsforschung und Reaktortechnik, FZ Jülich
Anwendung von Computercodes bei der Vorbereitung und Auswertung von Experimenten zum Spaltproduktverhalten in Reaktoren
15.05.1992

F. Geiss
Umweltinstitut der Gemeinsamen Forschungsstelle der EG, IRC Ispra
Forschungsschwerpunkte am Umweltinstitut der Gemeinsamen Forschungsstelle der EG
29.06.1992

K.-H. Naumann
KF Karlsruhe
Dynamische Eigenschaften fraktaler Aerosole
05.11.1992

H. Filthuth
Fa. Berthold, Bad Wildbad
Bildhafte Darstellung von Radioaktivitätsverteilungen
11.11.1992

P. Benes
Ceske Vyske Uceni Technike v Praze, Praha, CSR
The Institute of Nuclear Chemistry
Workshop Radiotracers in Biosystems, 10./11.12.1992

T.Elbert
UNBR CSAV, Praha, CSR
Profile of the UNBR CSAV
Workshop Radiotracers in Biosystems, 10./11.12.1992

A. Jegorov
Galena s.p. Research Unit, Ceske Budejovice, CSR
Profile of Galena s.p., A Research Unit in Ceske Budejovice
Workshop Radiotracers in Biosystems, 10./11.12.1992

K. Kopicka
NRI, Praha, CSR
The Nuclear Research Institute Rez
Workshop Radiotracers in Biosystems, 10./11.12.1992

L. Kronrad
UVVVR, Praha, CSR
The UVVVR Praha
Workshop Radiotracers in Biosystems, 10./11.12.1992

L. Leseticky
Charles University,Praha, CSR
The Institute of Organic and Nuclear Chemistry of the Charles University
Workshop Radiotracers in Biosystems, 10./11.12.1992

Z. Plecita
SUKL, Praha, CSR
The State Institute for Drug Control Praha
Workshop Radiotracers in Biosystems, 10./11.12.1992

V . PERSONNEL

Scientific Staff	Technical Staff	Postgraduate Students
Dr. L. Baraniak	B. Eisold	P. Fenger
Dr. G. Bernhard	J. Falkenberg	A. Roß
Dr. M. Bubner	H. Friedrich	
Dr. H.-J. Engelmann	Ch. Fröhlich	
Dr. H. Funke	G. Grambole	
Dr. G. Geipel	G. Heinz	
Dr. K.-H. Heise	H. Heyne	
Dr. S. Hübener	B. Hiller	
Dr. P. Merker	G. Hüttig	
C. Nebelung	R. Jander	
Dr. D. Rettig	P. Kluge	
Dr. M. Thieme [1)]	M. Meyer	
Dr. M.G. Stöbel [1)]	Ch. Müller	
W. Witke [1)]	H. Neubert	
Dr. H. Zänker	A. Rumpel	
	R. Ruske	
	H. Seifert [1)]	
	K. Wolf [1)]	

[1)] financed by BMFT-projects

VI. ACKNOWLEDGEMENTS

The Institute is a part of the Research Center Rossendorf Inc., which is financed by the Federal Republic of Germany and the Free State of Saxony on a fifty-fifty basis.

In addition, the Free State of Saxony provided support four projects covering the installation of modern equipment.
These projects were

- Investigations of the behaviour of gas borne pollutants (FZR-2)
- Measurement of natural radionuclides in rockpiles of uranium mining (FZR-10)
- Investigations on remobilisation of tracer pullutants in natural minerals by radiotracer techniques (FZR-11/14)
- Investigations on acid formation by autooxydation of sulfidic ores in rockpiles (FZR-16)

Five projects were supported by the Bundesminister für Forschung und Technologie.
The projects

- Investigations on Decommissioning of the Nuclear Facility AMOR-I of the Central Institute of Nuclear Research Rossendorf (CINR), BMFT 02 S 7370
- Investigations on the behaviour of gas borne pollutants
  * building up of the gas circulation "SPAREX", BMFT 03 ZFK 2015

were completed in 1992.
Three other projects are continued in 1993

- Development of methods for the determination of alpha active nuclides in building rubble, BMFT 02 S 74422
- Behaviour of radiotoxic pollutants in estates of uranium mining for a basis of remediation concepts, BMFT KWA 1231 4
- Chemistry of the heaviest elements
  * Gaschemical characterization of the element 106 as oxide or hydroxide BMFT 06 DR 101D

The DAAD-program PROCOPE has supported the contactation to the Centre d' Etudes Nucleaires de Cadarache, France.
The "Stifterverband für die Deutsche Wissenschaft" has enabled the partizipation on the ESTER-Workshop in Travedona, Italy.
The participation on a EG-project meeting was sponsored by the EG-GD XII - Brüssel.